Thesis for Degree of Master of Science

Study on characteristics of gas migration in the engineering barrier during the initial evolution process of the spent nuclear fuel (SNF) repository in Korea

by

Danu Kim

Division of Earth Environmental System Science

(Major of Earth and Environmental Sciences)

The Graduate School

Pukyong National University

February 2023

Study on characteristics of gas migration in the engineering barrier during the initial evolution process of the spent nuclear fuel (SNF) repository in Korea

(국내 사용후 핵연료 처분장 초기 진화과정 동안 공학적 방벽 내부에서의 가스 거동 특성 연구)

Advisor: Prof. Minhee Lee

by

Danu Kim

A thesis submitted in partial fulfillment of requirements
for the degree of Master of Science

Division of Earth Environmental System Science
(Major of Earth and Environmental Sciences)
The Graduate School
Pukyong National University

February 2023

Study on characteristics of gas migration in the engineering barrier during the initial evolution process of the spent nuclear fuel (SNF) repository in Korea

A thesis

by

Danu Kim

Approved by:

(Chairman) Minjune Yang

(Member) Sookyun Wang

(Member) Minhee Lee

February 17th, 2023

CONTENTS

LIST OF FIGURES

LIST OF TABLES

Study on characteristics of gas migration in the engineering barrier during the initial evolution process of the spent nuclear fuel (SNF) repository in Korea

Danu Kim

Division of Earth Environmental System Science
(Major of Earth Environmental Sciences)
The Graduate School
Pukyong National University

Abstract

The deep geological disposal has been studied as one of the most effective ways to permanently isolate the spent nuclear fuel (SNF). Due to the use of many nuclear power plants and the resulting saturation of temporary storage facilities, the construction of repository to permanently dispose the SNF and related researches and technology development are very urgent. The deep geological disposal is composed of the semi-permanently burying copper storage containers with SNF in the multiple barrier system designed with the natural barrier and the engineering barrier, which can prevent the outflow of radioactive nuclides to the biosphere. The gas could be generated from the continuous nuclear fission of the SNF and the geochemical and biological reaction in the canister and the barrier after the SNF was disposed in the repository. The gas migration may affect the nuclide migration in the barrier and finally affect the safety of the repository site. In this

study, laboratory experiments were performed to simulate the gas migration in the unsaturated engineering barrier during the early stage of the geological evolution of the SNF repository. The mixed gas (0.03% H_2 + 99.97% N_2) and the compacted bentonite core (1.67 g/cm^3 of dry bulk density, 4.5 cm in diameter and 3 cm in height) were used in experiments. Five parameters (the injection gas pressure, the water content, the confining pressure, the dry bulk density and the total pore pressure) influencing the gas migration in the engineering barrier were set by simulating the early stage of the SNF repository evolution process. Column experiments were performed to simulate gas migration in the dry engineering barrier medium at the SNF repository. Pressure breakthrough curves and concentration breakthrough curves on the gas phase in the compacted WRK bentonite core for each parameter were obtained from experiments. The average migration velocity in the core was calculated by using the data obtained through the breakthrough curves, and the effective gas permeability under certain core conditions was also calculated by considering the slip effect through the Klinkenberg correction.

The injection gas pressure on the surface of the compacted WRK bentonite core refers to the generation and inflow of gas inside the engineering barrier of the SNF repository. When the injection gas pressure at the barrier boundary becomes higher than that of the pore pressure of the barrier medium, the gas can migrate into the core in this study and be dispersed out through the SNF repository. Injection gas pressure conditions were applied by setting the $\triangle P$ (the pressure difference between the injection pressure and the total pore pressure in the core) to 0.02, 0.1, 0.3, 0.5 and 1.0 MPa. The average gas

migration velocity in the compacted WRK bentonite core increased 25 times when the injection gas pressure increased 50 times. The k_{eff} calculated by using the injection pressure and the pore pressure exhibited the typical Klinkenberg effect, proportional to the reverse of the pressure difference ($\triangle P$). The gas permeability modified by the Klinkenberg correction (k_∞) increased by 1.8 times when the injection gas pressure increased by 10 times. The pressure is proportional to the ratio of velocity to permeability but when the pressure increased 10 times, the ratio of velocity to permeability increased 7 times in this study. This difference may result from that the Klinkenberg correction can't reflect the gas flow in the transition flow regime for the experiment.

The water content is a parameter that controls the pore space in the engineering barrier of the SNF repository. Laboratory scale experiments were performed under the conditions of 4.3, 7.8, and 13.1% water content. As the water content in the core increased from 13.1% to 4.3%, the gas migration velocity and the modified gas permeability (k_∞) increased by 2 and 2.7 times, respectively. This is because the reduction of the water content in the buffer increases the pore space and increases the gas migration velocity. Results supported that when the engineering barrier is dry due to the heat released from the Cu-canister during the early evolution of the SNF repository, the gas can migrate into the engineering barrier very fast (36~72 cm/hour).

The confining pressure is the pressure applied at the outer wall of the engineering barrier buffer, gradually increasing from the atmospheric pressure to higher than the hydrostatic pressure generated at the depth of the SNF repository. In this study, the average

gas migration velocity and the k_∞ at the condition of the confining pressures of 1, 5, 10 and 20 MPa were calculated. From the breakthrough curves from experiments, the average gas migration velocity increased to about 6.7 times faster and the k_∞ increased by 6 times over as the confining pressure decreased by 20 times. The increase of the average gas migration velocity and the k_∞ by the confining pressure decrease showed almost identical patterns.

The dry bulk density is one of the physical properties of the compacted bentonite core (a buffer medium of the engineering barrier), affecting the durability, the k_∞, and the swelling pressure of the engineering barrier. Cores having 4 different dry bulk densities of 1.67, 1.74, 1.78 and 1.84 g/cm^3 were used in the gas migration experiments. The average gas migration velocity according to the dry bulk density decreased by up to about 9.5 times (from 3.4 to 32.7 cm/hour) as the dry bulk density increased from 1.67 to 1.84 g/cm^3. The k_∞ also decreased by up to about 11 times (from 5.51×10^{-17} to 6.22×10^{-16} m^2) as the dry bulk density increased. However, the ratio of the k_∞ to the average gas migration velocity was not consistent with the bulk density decrement. This is because of the difference in the gas flow regime of the core due to the decrease in the average pore diameter size.

The total pore pressure in the core is the sum of the hydrostatic pressure, the bentonite expansion pressure and the partial pressure increased by the water vaporization. In this experiment, the injection gas pressure was different at 0.53, 1.03, 3.03, 5.03 and 7.03 MPa, but the $\triangle P$ was maintained at 0.3 MPa (pore pressure: 0.50, 1.00, 3.00, 5.00 and 7.00 MPa). From the breakthrough curve of the gas in the core, there was very little difference in the gas migration velocity due to the pore pressure difference, but the gas

dispersivity in the core clearly decreased as the pore pressure in the core increased. This means that even if the pore pressure is high in the unsaturated engineering barrier, the gas migrates at the same velocity if the $\triangle P$ is constant.

From the experimental results, the average gas migration velocity and the Klinkenberg's corrected gas permeability (k_∞) for the compacted WRK bentonite core at the unsaturated condition were in the range of 3.0 ~ 90.0 cm/hour and in the range of 2.31 $\times$ 10^{-15} m^2 ~ 5.51 $\times$ 10^{-17} m^2, respectively. Through this study, it is suggested that the gas migrate at a very high velocity in the engineering barrier, which is unsaturated during the early stage of the SNF repository evolution process and it is important to control safely the Cu-canister and the engineering barrier during the early stage of the SNF disposal because of the fast gas migration in the engineering barrier.

Keywords: Spent nuclear fuel repository, Gas generation, Gas migration, Engineering barrier, Gas permeability, Klinkenberg effect, Knudsen number

CHAPTER 1. INTRODUCTION

After the Industrial Revolution, a large amount of carbon dioxide (CO_2) was emitted into the atmosphere due to the increase in the use of fossil fuels, and the increase of the CO_2 concentration in the atmosphere caused the global warming. By adopting the Paris Agreement to address the global warming, many countries are trying to reduce the Earth's temperature rise rate by reducing greenhouse gas emissions, including the CO_2 (An et al, 2018). Therefore, various renewable energies have been studied as an alternative to fossil fuel energy, which accounts for the largest proportion of greenhouse gas generation and emission causes (Figure 1).

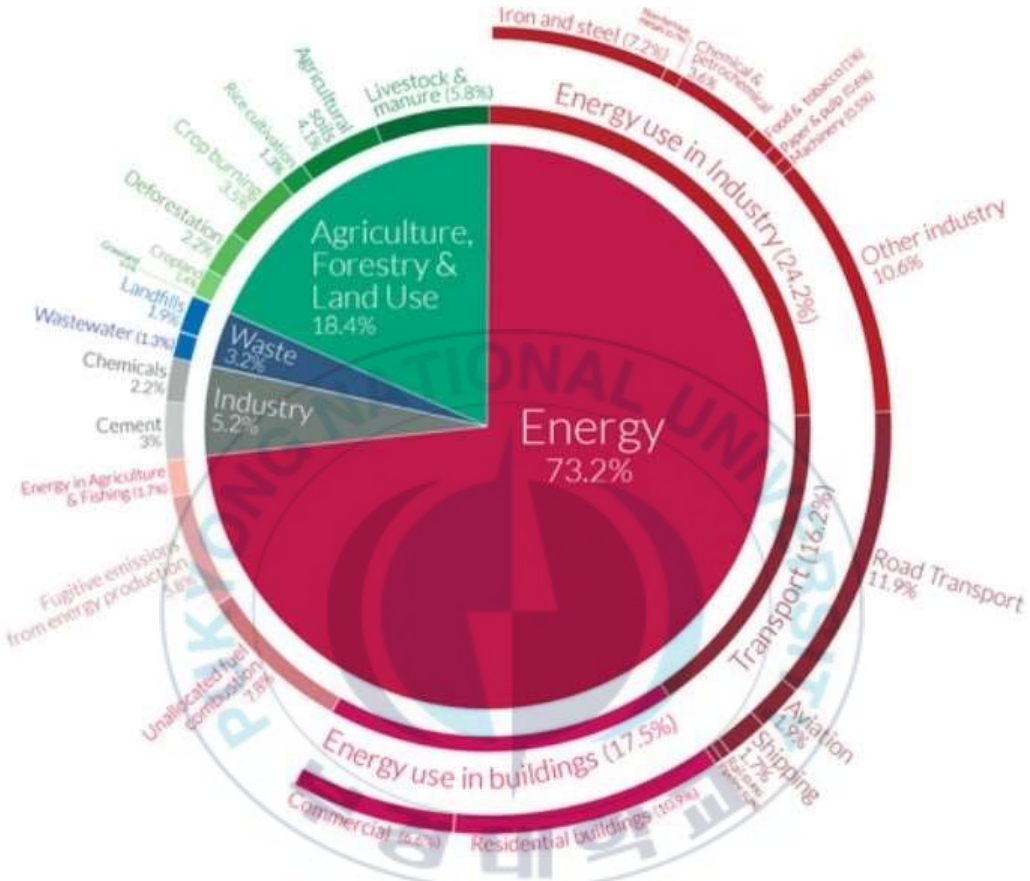

Fig. 1. Greenhouse gas emissions by sector (Ritchie, H. 2020).

Nuclear power is the cheapest among the various renewable energy sources and generates very little carbon (1% of the carbon generation of fossil fuels) (Lee, 2006). According to the average settlement price of electricity traded on the Korea Electric Power Exchange in 2012, the oil is the highest at 250.72 won per kWh, followed by a pumped storage hydropower of 213.93 won, a hydraulic power of 180.86 won, natural gas of 168.10 won, and bituminous coal of 66.25 won, and the nuclear power is the lowest at 39.52 won

(Lee, 2013). In 2022, over 400 nuclear power plants are currently in operation worldwide (Figure 2). South Korea has 24 nuclear reactors, accounting for about 27.4% of its total electricity production and ranked 5th in the amount of nuclear power plants in 2021

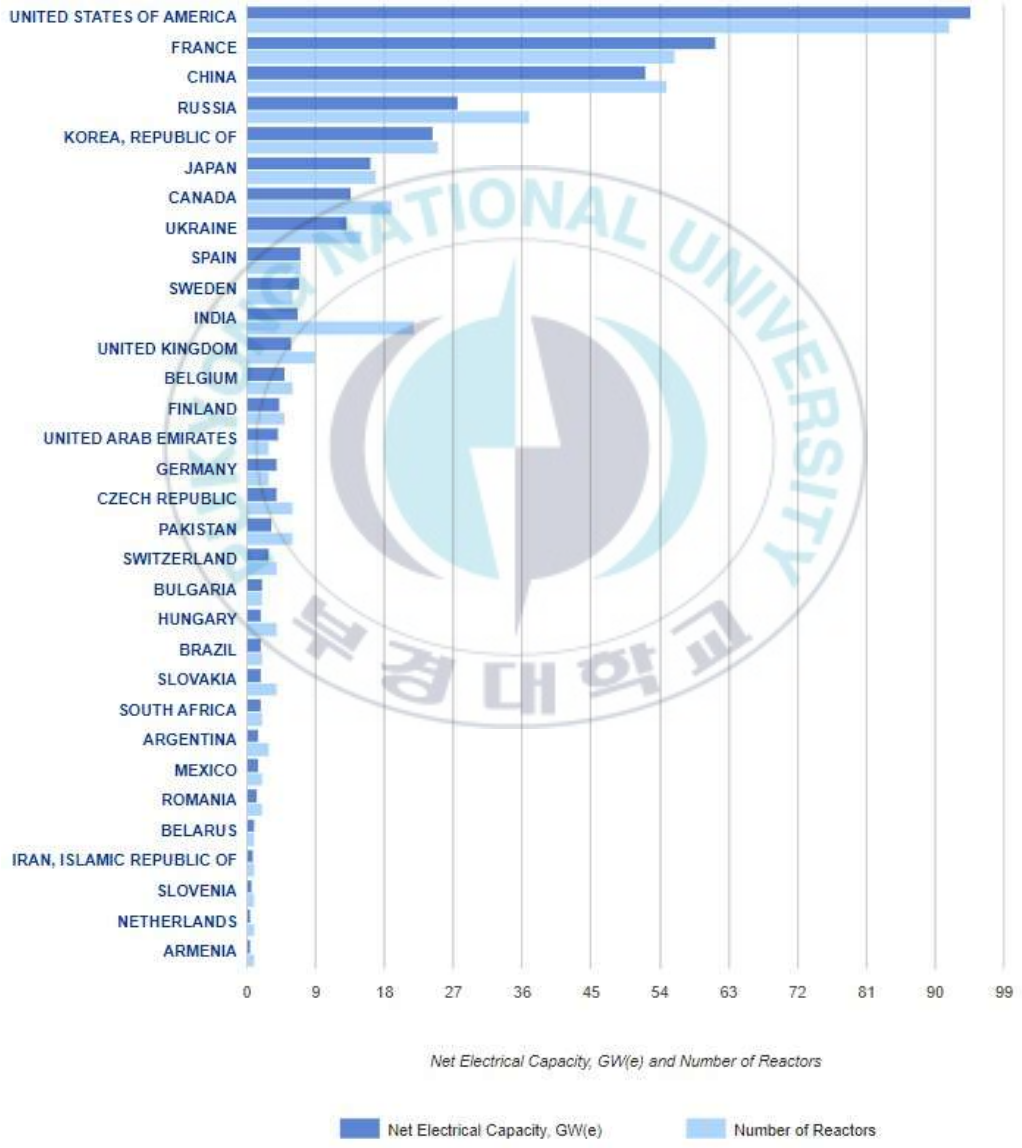

Fig. 2. Nuclear power plant operations in the world (IAEA, 2022)

(IAEA,2022).

However, nuclear power has the fatal disadvantages as well as its advantages. In the process of nuclear power generation, a great deal of radiation is emitted, and when exposed to radiation by an accident, as in Fukushima or in Chernobyl, serious environmental damages may occur. Radiation is also originated from radioactive fuel wastes left after the nuclear power generation. Radioactive wastes in the power plant are classified according to how much the heat or the radiation are released, and the radioactive waste that generates high-temperature heat (> 2 kW/m^3) and releases high radioactive concentrations (> 4,000 Bq/g) is called as the high-level waste (HLW). HLW is mainly associated with the generation of nuclear power and the production of nuclear weapons. The HLW in the nuclear power generation is either the spent nuclear fuel (SNF) or the radioactive material remaining after reprocessing of the SNF (NRC, 2012). Most of the HIW generated in Korea is the SNF generated during the operation of nuclear power plants and is currently being stored in temporary storage facilities on the site of nuclear power plants. In 2021, the temporary storage facilities except the Saeul site were almost saturated (> 60%) and in particular, the saturation ratio of the temporary storage facilities in Wolseong was 98.8% (Figure 3) (Korea Hydro & Nuclear Power, 2021). Therefore, it is very important to come up with a plan to permanently dispose of the large amount of SNF located at temporary storage facilities on nuclear power plants.

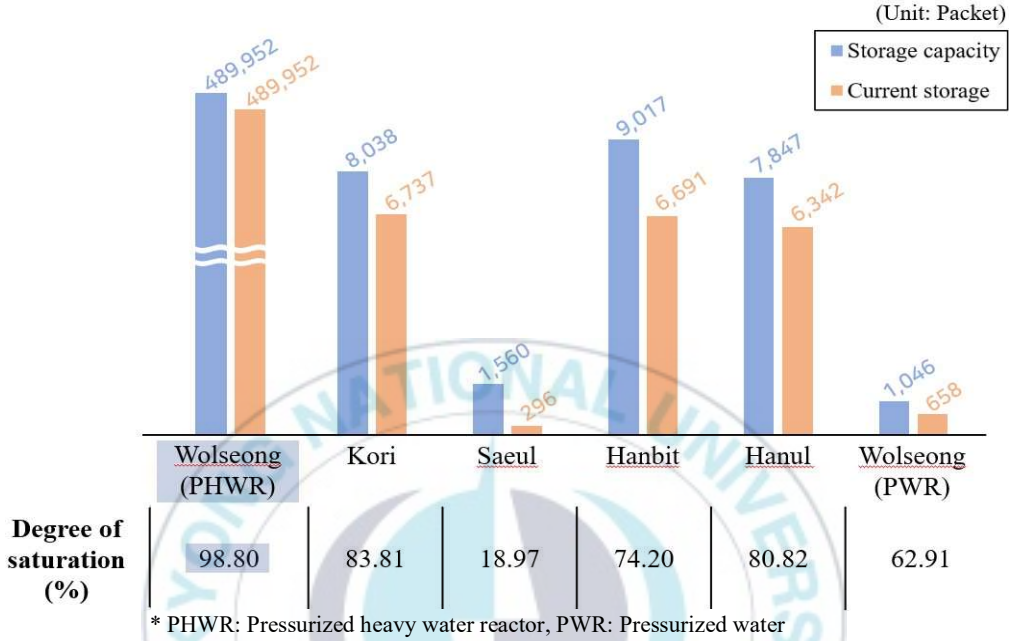

Fig. 3. Status of spent nuclear fuel storage in Korea (from Korea Hydro & Nuclear Power, 2021).

The use of nuclear power has continued not only in Korea but also around the world, and there have been many discussions on how to dispose of the HLW. A wide variety of long-term disposal options have been considered over the past few decades, including sending the HLW into the outer space and reprocessing the SNF to the new nuclear fuel (NRC, 2001a; Hamilton et al, 2012). But most of them have not been implemented because of safety issues, cost and environmental pollutions. The subsurface disposal of the SNF includes the burial in the depths of the bedrock, placing HLWs within the ice sheet of Antarctica (Hebel et al, 1978), subsea treatment (Hamilton et al, 2012; NRC, 2001b; NWMO, 2005; North, 1997), burials under the island, etc (Hamilton et al, 2012; NRC,

2001b; NWMO, 2005). Among them the deep geological disposal is currently most studied worldwide because it is considered as an effective storage technology, preventing the leakage of radionuclides for a long time by selecting a geologically stable underground bedrock. The basic concept of the deep geological disposal is to store the HLW in the multiple barrier system including engineering barriers consisting of canisters, buffers, and backfill materials and geologically stable natural barrier (Figure 4).

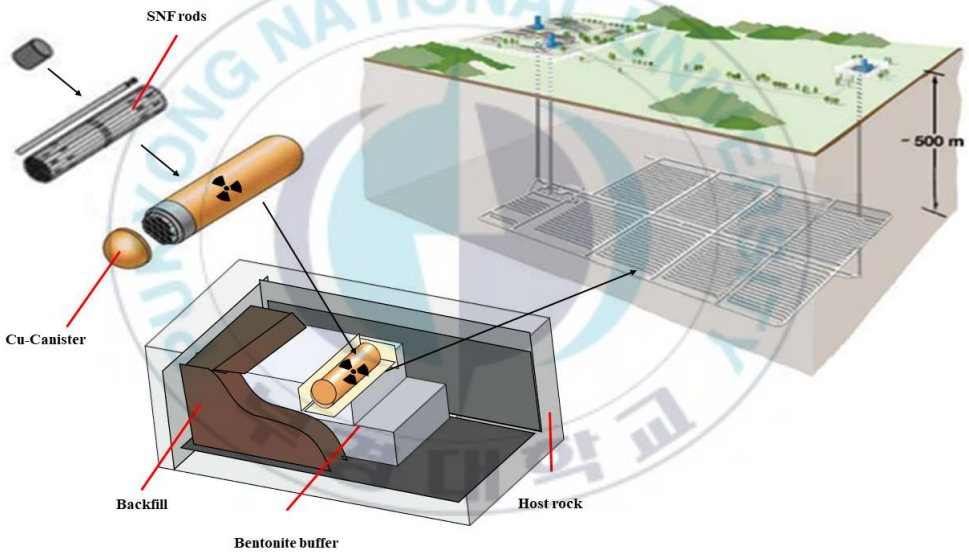

Fig. 4. Schematic of the deep geological disposal.

The most representative disposal site design is the KBS-3 type developed by the Swedish nuclear fuel waste management company SKB (Svensk Kärnbränslehantering AB) (Lee et al, 2007). The energy and the heat generated by nuclear fission and the radioactive decay of the SNF rods were reduced in the temporary storage (dry and wet storage) site for a few years. After fixed the SNF rod assembly (bundle) to the cast iron, they were sealed

in a copper canister in a thickness of about 5-10 cm and each canister was stored in a vertical/horizontal disposal cavity with the engineering barriers (composed of compacted bentonite blocks). When all of storage cavities are filled with cu-canister, the empty area in the disposal site is filled with back-fill materials and the disposal site is sequentially closed.

After the disposal site is closed, the environment of the multiple barrier system in the disposal site is affected by various thermal-hydraulic-geochemical reactions, such as the heat transfer from storage containers, the saturation of groundwater, the swelling due to expansion of the bentonite buffer, and the stress from the host rock. During the hydrogeological evolution of the disposal site, various gases could be generated inside the disposal site, and if the gases are accumulated in the SNF repository and leak into the surface, fatal radioactive nuclides may also disperse together. The evolution of the SNF repository according to the gas-nuclide migration will be described in detail in Chapter 3. In particular, radioactive nuclides can migrate very quickly if the engineering barrier that has not yet been saturated is damaged due to natural disasters after the disposal is completed.

In this study, the gas migration inside the unsaturated engineering barrier of the SNF disposal site was simulated in the laboratory scale, focusing on the effect of gas on the nuclide migration caused by the damage of the engineering barriers such as natural disasters or unexpected accidents.

CHAPTER 2. OBJECTIVES

Objectives of this study are (1) to quantitatively identify the gas migration characteristics in the engineering barrier during the early evolution stage of the SNF repository and (2) to calculate the gas permeability of the unsaturated engineering barrier material (the compacted bentonite core) and to measure the gas migration velocity in the core through laboratory scale experiments.

This study was mainly divided by three parts listed below.

1. Laboratory scale experiments were designed to simulate the gas migration at various engineering barrier conditions during the early stage of the SNF repository.

2. Gas migration characteristics were quantified by obtaining the gas breakthrough curves from experiments, and main influential parameters to control the gas migration in the engineering barrier of the SNF repository were also determined.

3. Gas permeabilities of the engineering barrier at various barrier and repository conditions, representing the early stage of the SNF repository, were calculated by using experimental results.

CHAPTER 3. BACKGROUND

3.1. Previous studies

3.1.1. Gas generation in the repository

Because the SNF repository design in Korea has not yet been determined, the information of gas generation and migration in the multiple barriers of the Korean SNF repository is very limited and the gas-related studies in the SNF repository have been dependent on the reference data from previous overseas studies. Domestic research related to the SNF repository began with the construction of mid- and low-level radioactive waste (M&LLW) disposal sites at Gyeongju in the early 2000s (Kim et al, 2010a, Kim et al, 2010b). However, they focused on the changes in the hydrogeological environment around the M&LLW repository in the shallow depth (80-130 m). Park et al. (2010) reviewed the gas generation mechanisms in the domestic M&LLW repository. The effect of generated gas on the geochemical and biological environments in the M&LLW repository were investigated through the geochemical modeling (Choung et al, 2014). Recently, Ahn et al. (2019) evaluated the long-term safety and the risk of the M&LLW repository in relation to the gas generation and migration in the engineering barrier of the repository. However, these previous studies mainly summarized the gas generation mechanisms based on results of previous studies in abroad and did not reflect the actual environment of the SNF repository in Korea because most researches were limited to the M&LLW environment. There exist only a few domestic studies for the gas generation by the geo-biological activity,

even in conceptual levels.

Overseas research on the deep geological disposal for the SNF began in the 1990s. It was studied that various gas could be generated or introduced due to different reasons such as the corrosion of Cu-canister, the continuous nuclear fission in the SNF, and the microbial activity in barrier media (Bond et al, 1997; Wikramaratna et al, 1993). For the H_2 gas as the main gas produced in the repository, its generation mechanism due to the of oxidation of the copper canister surface under aerobic condition in the early repository stage was described (King et al, 2013). It was also reported that when the sulfide reaches the surface of the canister due to the reduction of sulfate by microorganisms in the repository, the H_2 gas could be generated (King et al, 2011; King et al, 2021). In addition, Cl^- and HS^- exist naturally in groundwater and HS^- generated by microbial activity through the buffer could promote dissolution of copper, causing the H_2 gas generation, and this corrosion reaction could be accelerated when the pore water is brine water (King et al, 2011; King et al, 2013). By the free radical production of water molecule by gamma rays generated from the radioactive decay of the SNF, the H_2 gases may be produced. Methane (CH_4) gas can also be produced from various processes such as the microbial activity in geological environments near the surface, the reduction of dissolved CO_2 in deep crust environments, the magma degeneration, etc (Pitkänen and Partamies, 2007). Methane in the SNF repository can produce HS^- and H^+ in water through anaerobic oxidation by sulfate and iron (Whiticar, 1999). Main mechanisms and reactions related to the H_2 gas generation and consumption in the SNF repository are summarized in Table 1.

Table 1. Possible H_2 production and consumption mechanisms in SNF repository.

Mechanism		Chemical equation	Note
Corrosion of cast-iron insert	Aerobic condition	$4Fe + 6H_2O + 3O2 \rightarrow 4Fe(OH)_3$	
	Anaerobic condition	$Fe + 2H_2O \rightarrow Fe(OH)_2 + H2$ $3\ Fe(OH)_2 \rightarrow Fe_3O_4 + 2H_2O + H_2$	Various ferrous salts can be created
Corrosion of copper canister	Reduction environment	$Cu + Hs^- \rightarrow Cu(HS)_{ADS} + e^-$ $Cu + Cu(HS)_{ADS} + HS^- \rightarrow Cu_2S + H_2s + e^-$	Anodic reaction
		$2HS^- + 2e^- \rightarrow H_2 + 2S^{2-}$ $H_2O + e^- \rightarrow 1/2H_2 + OH^-$	Cathodic reaction
Water radiolysis		$H_2O \rightarrow 2H\cdot + O\cdot$ $2H\cdot \rightarrow H_2$	
Serpentinization of olivine		$6Mg_{1.8}Fe_{0.2}SiO_4 + 8.2H_2O \rightarrow 1.8Mg(OH)_2 + 3Mg_3Si_2O_5(OH)_4 + 0.4Fe_3O_4 + 0.4H_2$	
Sulfate reduction reaction		$Propionate + 0.75SO_4^{2-} \rightarrow Acetate- + HCO^{3-} + 0.75HS^- + 0.25H^+$	
		$Butyrate- + 0.5SO_4^{2-} \rightarrow 2Acetate- + 0.5HS^- + 0.5H^+$	
Acetic acid production reaction		$Propionate- + 3H_2O \rightarrow Acetate^- + HCO_3^- + H^+ + 3H_2$	
		$Butyrate- + 2H_2O \rightarrow 2Acetate^- + H^+ + 2H_2$	
		$Lactate- + 2H_2O \rightarrow Acetate^- + HCO_3^- + H^+ + 2H_2$	

* modified from King and LeNeveu, 1992; King et al, 2011; McCollom et al, 2016; Muyzer and Stams, 2008; Thauer et al, 1977; Wada et al, 1995; Wersin et al, 1994

3.1.2. Gas migration in the multiple barrier

Research on the gas migration in the domestic SNF repository began in the early 2000s. In 2007, the Korea Atomic Energy Research Institute (KAERI) installed an engineering-scale experimental device (KENTEX) to study the engineering barrier for the domestic SNF repository system (Lee and Cho, 2007) and empirical experiments were

performed to identify the thermal-hydro-mechanical (THM) properties of the compacted bentonite block as the engineering barrier (Kwon and Cho, 2011; Lee et al, 2019). In 2008, the KAERI participated in the international joint study of DECOVALEX (Development of COUPLED MODELS and their VALIDATION AGENT) Phase 4, and various researches such as crack representation by heating and gas pressure, and investigation of gas migration in the clay layer and bed rock formation have actively conducted (Kim et al, 2021).

In the case of foreign countries, researches on the gas migration in the deep geological repository were conducted in European countries that planned to build the HLW repository in the late 1990s. Representatively, through the FORGE (Fate Of Repository GasEs) project in Europe, the effects of gas generation and migration in engineering barrier systems on the safety of the SNF repository were studied through large-scale gas injection tests (Sellin, 2014; Shaw, 2015). In six countries (GAMBIT club; Sweden, Switzerland, Spain, Japan, France and Finland), a total of three stages of research on the gas migration in natural and engineered barrier systems were conducted, but there exist many limitations to understanding the gas migration and mechanisms due to uncertainty (Nash et al, 1998; Hoch et al, 2004). When the gas generated from the SNF repository is accumulated in voids in engineering barriers or host rock, it is possible to move through microcracks inside barriers and to generate additional fractures in barriers (Horseman et al, 1999; Sellin and Leupin, 2013). Studies on the gas transfer process in low permeability clay materials were also performed (Marschall et al, 2005; Cuss et al, 2014). Davis and Selvadurai (2005) studied the hydrodynamic state change of clay media by the gas (aligning clay particles in the direction of dispersion in the medium due to expansion, increasing plastic deformation)

when the gas pressure reaches the reference stress level acting on the clay medium during the gas accumulation. Currently, the most active international study for the gas is of the DECOVALEX project, which includes diverse experimental and numerical studies such as evaluating disposal system safety and predicting migration within engineering barriers and designing the complex thermal-repair-mechanical-chemical (THMC) migration simulation in the SNF repository (Kim et al, 2021). However, most of these preceding studies have been performed on saturated conditions of the barrier, and studies on unsaturated (or partially saturated) barrier condition have not been conducted.

3.2. Scenario of the gas migration in the engineering barrier according to the evolution process of the SNF repository

The geological and physicochemical environments of the multiple barrier in the SNF repository change as the SNF repository time goes by, and various gases are generated in the SNF repository. This evolution process of the multiple barrier system could be subdivided into several steps according to the characteristics of the gas generation and migration (Figure 5). For each evolution stage of the SNF repository based on the gas generation and reaction, the main mechanism of the gas migration in the multiple barrier of the SNF repository was described in this study.

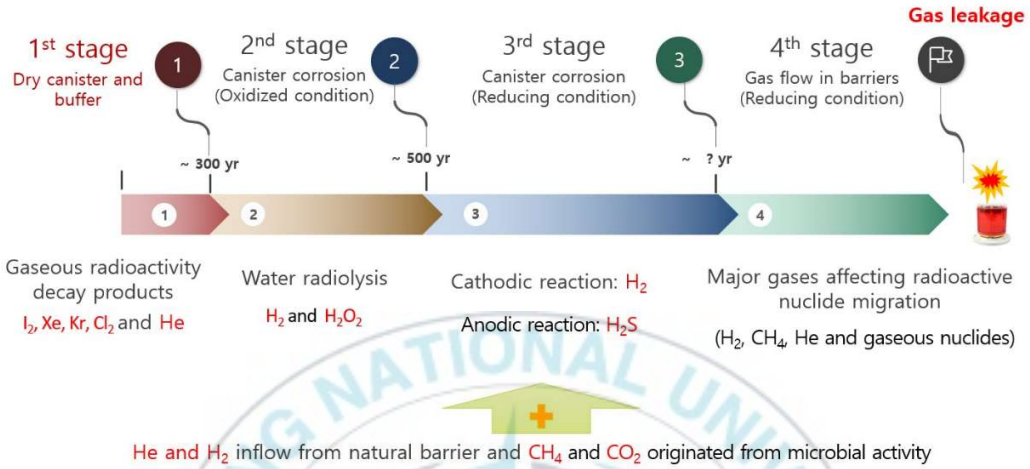

Fig. 5. Evolution process of the SNF repository and gas generation mechanism for each evolution stage.

- Stage 1: The initial stage of the SNF repository (over approximately 100 years after storage)

In stage 1, the surface of the canister maintains a high temperature (Figure 6) by the heat released by the radioactive decay in the SNF and the engineering barrier around the canister is kept unsaturated. If the canister is fractured or the cracks in the barrier occur due to the external environment, the gas starts to move in the unsaturated barrier medium by advection and dispersion according to the pressure gradient. Thus, Darcy's law (Equation 1) can be applied to the gas migration because the swelling pressure of the entire medium is not applied to the unsaturated barrier medium (usually compacted bentonite core) (Li et al, 2016).

$$Q = KA\frac{\Delta P}{\mu L} \quad (1)$$

Where Q is the total flow rate (volume of fluid as a function of time, m^3/s); K is the permeability of fluid (m^2); A is the cross-section area of the fluid-flowing barrier medium (m^2); μ is the pressure gradient (Pa); is the gas dynamic viscosity (Pa · s); L is the distance of the fluid-flowing barrier medium (m).

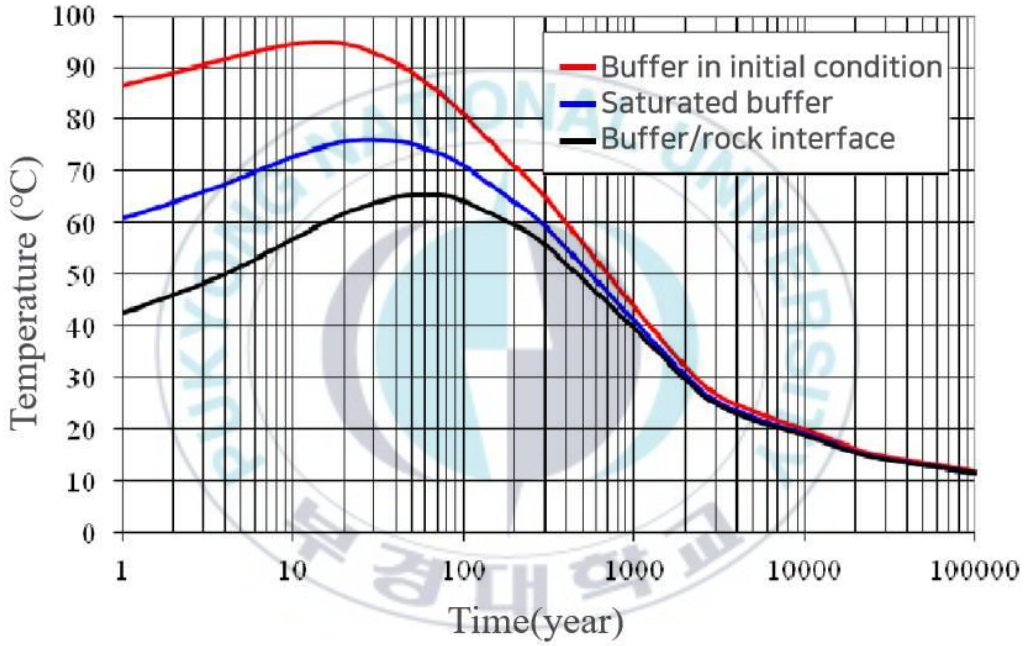

Fig. 6. Variation of temperature at the engineering barrier of the SNF repository (POSIVA, 2012).

- Stage 2: The stage in which the barrier medium is fully saturated with water

The amount of heat and radiation emitted by fission products decreases rapidly, lowering the temperature around the canister, and groundwater flows in from the host rock. Then the voids of the buffer and backfill are converted to the saturation environment. During the repository construction, the aerobic environment is maintained (O_2 in the

repository is dissolved in groundwater), and the canister can be corroded by the oxidation reaction of the copper canister surface in contact with groundwater even if the canister is not ruptured due to the external environment. In order for gas to be injected into the saturated buffer, the total injection gas pressure generated by canister corrosion and continuous radiation must exceed the total pore pressure combined with the pore water pressure and the expansion pressure of the barrier. In an environment immediately after the buffer is saturated, but the bentonite is not fully expanded (swelling of clay minerals), so the generated gas migrates by pushing the water filled in the buffer pores (viscous-capillary flow) when the gas pressure is very high. After the buffer is saturated, if the total injection gas pressure is lower than the total pore pressure, the gas is partially dissolved depending on solubility and slowly moved inside the barrier medium for a long time by diffusion mechanism in groundwater.

- Stage 3: The stage maintaining the reducing environment in the multiple barrier

As the O_2 is consumed by the corrosion reaction of the Cu-canister, the SNF repository is converted into a reducing environment. In a reducing environment, HS^- present in groundwater plays an important role in generating gas in engineering barriers. The H_2, H_2S and CH_4 gas can be generated or consumed by the dissolution of copper metal on the surface of the canister, the mineral precipitation and the microbial decomposition reaction at the reducing environment. However, the bentonite in the engineering barrier expands completely and builds a high total pore pressure in the buffer. Thus, most of the generated gases are captured in the pore spaces of the barrier and they slowly dissolve into pore water because of the high pore pressure. Therefore, the gas migration in the barrier is

mainly controlled by the diffusion of the dissolved gas phase in pore water. If the gas concentration in pore water reaches to the solubility, the gas is captured as the bubble type in the pore space until it migrates through the new pathway in the barrier. At very high gas injection pressure condition, the gas is likely to move into the compacted bentonite barrier through the dilatant pathway rather than by the viscos-capillary flow that pushes water filled in void spaces of the barrier (Marschall et al, 2005).

- Stage 4: The stage in which the gas reaches the outer boundary of the barrier in the SNF repository

As the final step in the SNF repository evolution process, when the entry pressure of gas generated from the barrier inside exceeds the total pore pressure in the multiple barrier, the free gas phase may be leaked to the outside and/or the dissolved gas may reach to the outside.

Laboratory scale experiments to simulate the gas migration in the engineering barrier at the early stage of the SNF repository environment were performed in this study. For experiments, the WRK compacted bentonite core as the engineering barrier material was used and the unsaturated barrier condition was applied to represent the early stage of the SNF repository evolution process. Assuming the abrupt gas leakage from the Cu-canister damage by the external force, the characteristics of gas migration into the engineering barrier were investigated by interpreting various gas breakthrough curves and the change of gas permeability in the barrier due to the different barrier conditions was also discussed in this study.

3.3. Bentonite as a buffer material

Bentonite is one of the swelling claystone consisting mostly of montmorillonite belonging to the smectite group, which is formed mainly by the weathering of volcanic ash (< 2 μm in diameter) (Lexico, 2021). Bentonite also has the ability to sorb large amount of water molecules on the interlayer spaces, increasing its volume several times over. The 2:1 layer unit of montmorillonite (the main phyllosilicate structure of bentonite) consists of one aluminum octahedron layer between two silica tetrahedron layers, and some of the central Si^{4+} and Al^{3+} ions in the silica tetrahedron or in aluminum octahedron layers are replaced by Al^{3+} and Mg^{2+} ions. The negatively charged parts due to this substitution are electrically balanced by absorbing cations (Na^{+}, Mg^{2+}, Ca^{2+}, etc.) on the surface of interlayers (Karnland, 2010). Montmorillonite is divided into the Na-type bentonite and the Ca-type bentonite according to the main type of exchangeable cation present between layers of the montmorillonite (Ca or Na). The swelling property of the bentonite has advantage in groundwater sealants and can serve to seal spaces on the barrier boundaries (for example, the gap between Cu-canister and the compacted bentonite block or between bentonite blocks) and to prevent the gas or groundwater flow passing through the barrier cracks or gaps. The interlayer phyllosilicate structure of bentonite has very large surface area, making a valuable adsorbent to minimize the radionuclide migration in the SNF repository. In previous studies, several types of bentonites such as MX-80, Kunigel- V1 and FEBEX were used as the possible material for the engiennering barrier (the compacted

bentonite block) (Karnland, 2010; Kohno et al, 2018; Wilson, 2017). In this study, the WRK bentonite purchased from the Inner Mongolia region in China was used to manufacture the compacted bentonite core as the engineering barrier block for experiments. The properties of the WRK bentonite core were described in Chapter 4.

3.4. Gas permeability of bentonite core

Gas permeability is the parameter, which refers to the property of the medium to the fluid flowing into the porous medium by the pressure gradient and is used as an indicator of how well the gas passes through the medium (Lee et al, 2000). Gas permeability is divided into three types: the intrinsic permeability (k_{ig}), the effective permeability (k_{eff}), and the relative gas saturation ratio (k_{rg}). The k_{ig} is an inherent property independent of the pressure applied to the specimen and refers to the permeability when it is saturated with only one fluid (here of gas) in the porous medium, and in this study, it refers to the gas permeability of the bentonite core when the water content is 0%. When two fluids are present in the pore space (gas and water in this study), the permeability of each fluid in the porous medium depends on the saturation of the other fluid, which is called the k_{eff} (Villar et al 2014). Therefore, there is a difference between the k_{ig} and the k_{eff} depending on the water content in the gas–water fluid system. The ratio of the fluid saturation is the k_{rg} and the k_{eff} can be expressed as follows (Kim et al, 2013).

$$k_{eff} = k_{ig} \cdot k_{rg} \tag{2}$$

Where k_{eff} is the effective gas permeability (m^2); k_{ig} is the intinsic gas permeability (m^2); k_{rg} is the relative gas saturation ratio (0~1).

3.5. Gas slip effect

The study of gas migration through porous media has been studied for decades in the field of petroleum engineering. Since the use of oil and shale gas is still steady, many studies are being conducted to understand the fluid permeability of reservoir rocks for effective resource collection. The phenomenon of gas slip near the inner wall of each particle in the porous medium was first reported by Maxwell (1879). Afterwards, Knudsen (1909) extended the gas slip effect to the diffusion of gas and the collision with the inner wall of the medium, and Klinkenberg (1941) studied the effect of gas slip on the gas permeability in a porous medium. Klinkenberg argued that the gas permeability is a linear relationship with the inverse of the pressure due to the sliding of gas molecules on the surface of a porous medium. In general, the effect of Klinkenberg becomes important when the mean free path radius of the gas molecule is similar to the pore-throat radius (mean pore size in this study). The Klinkenberg effect depends on the magnitude of the dimensionless parameter called the 'Knudsen number', and the gas diffusion type varies with the Knudsen number. The definition and the usage of the Knudsen number to calculate the gas permeability of the compacted WRK bentonite core were described in detail in Chapter 4.

CHAPTER 4. MATERIALS AND METHODS

4.1. WRK bentonite

Bentonite consists of various silicate clay minerals such as montmorillonite, feldspar, quartz, cristobalite, etc, and it can be divided into 'Ca-type bentonite' and 'Na-type bentonite' according to the content of Ca and Na present in the montmorillonite. Bentonite used in this study was named 'WRK' and it was provided from the Korea Atomic Energy Research Institute (KAERI). It was purchased from the inner Mongolia Autonomous region in China and would be likely to be used as an engineering barrier material for the SNF repository in Korea.

4.1.1. XRD and XRF analyses

X-ray diffractometer (XRD; X'Pert-MPD, Philips) analysis was performed to determine the mineralogical composition of the WRK bentonite. Also, X-Ray Fluorescence Spectrometer (XRF; Shimadzu, XRF-1800) analysis was performed to observe the major chemical components and the bentonite type of the WRK bentonite.

4.1.2. Properties of the compacted WRK bentonite core

The WRK compacted bentonite core as the buffer material in the SNF repository site

was designed as a cylindrical shape (diameter of 4.5 cm; height of 3-5 cm) and was manufactured with different dry bulk densities (1.67-1.84 g/cm^3; the compaction load of 0.2 to 0.6 tons) for experiments. The physical properties of the WRK compacted bentonite cores were investigated and the results are shown in Table 2.

Table 2. The physical properties of the WRK bentonite core with different compaction load.

Properties (unit)	Definition	Compaction load (ton) applied to manufacture the bentonite core			
		0.2	0.4	0.5	0.6
Water content (%)	$w = m_w/m_s \times 100$	13.07	13.15	12.97	12.89
Density of solid (g/cm^3)	$\rho_s = m_s/V_s$	2.15	2.24	2.29	2.37
Dry bulk density (g/cm^3)	$\rho_d = m_s/V_t$	1.67	1.74	1.78	1.84
Wet bulk density (g/cm^3)	$\rho_w = m_t/V_t$	1.89	1.97	2.01	2.08
Degree of saturation	$S = V_w/V_p$	0.978	0.57	1.136	0.63
Porosity	$n = V_p/V_t$	0.223	-	0.203	0.376
Average pore diameter (nm)	-	28.4	24.6	22.3	21.7

* m_w : weight of water in the WRK bentonite core; m_s : weight of the WRK bentonite core after drying at 105℃; V_s : weight excluding voids in the WRK bentonite core; V_w : volume of water in the WRK bentonite core; V_p : volume of pore in the WRK bentonite core; V_t : total volume of the WRK bentonite core

4.2. Gas for the experiment

The main gases generated in the SNF repository are probably the H_2 and the He gas, and thus the H_2 gas was selected as the main gas phase for the gas migration study in the multiple barriers, considering its reactivity and production in the SNF site. The Korean Safety Manage Regulation approved the usage of the dilute H_2 gas mixed with less than 4%

of H_2 concentration in the laboratory without specific security facility. The appropriate detection range of the H_2 concentration detector used in the experiment was 0.001~0.005%. Therefore, the nitrogen gas (99.97%) mixed with 0.03% (300 ppm) of the H_2 gas was used to simulate the gas migration into the compacted bentonite core in this study.

4.3. Experiments for the gas migration in the engineering barrier

Laboratory scale experiments were performed to investigate the gas migration in the engineering barrier at the early stage of the SNF repository evolution process. Experimental apparatus was manufactured to simulate the underground environment of the engineering barrier at the early SNF repository stage. The experimental apparatus consists of the high-pressured syringe pump (Teledyne ISCO, 260D Syringe pump), the high-pressure stainless-steel cell, the gas tank, the backpressure regulator, the pressure regulator, the digital pressure gauge, the valves, the H_2 gas concentration detector, etc (Figure 7).

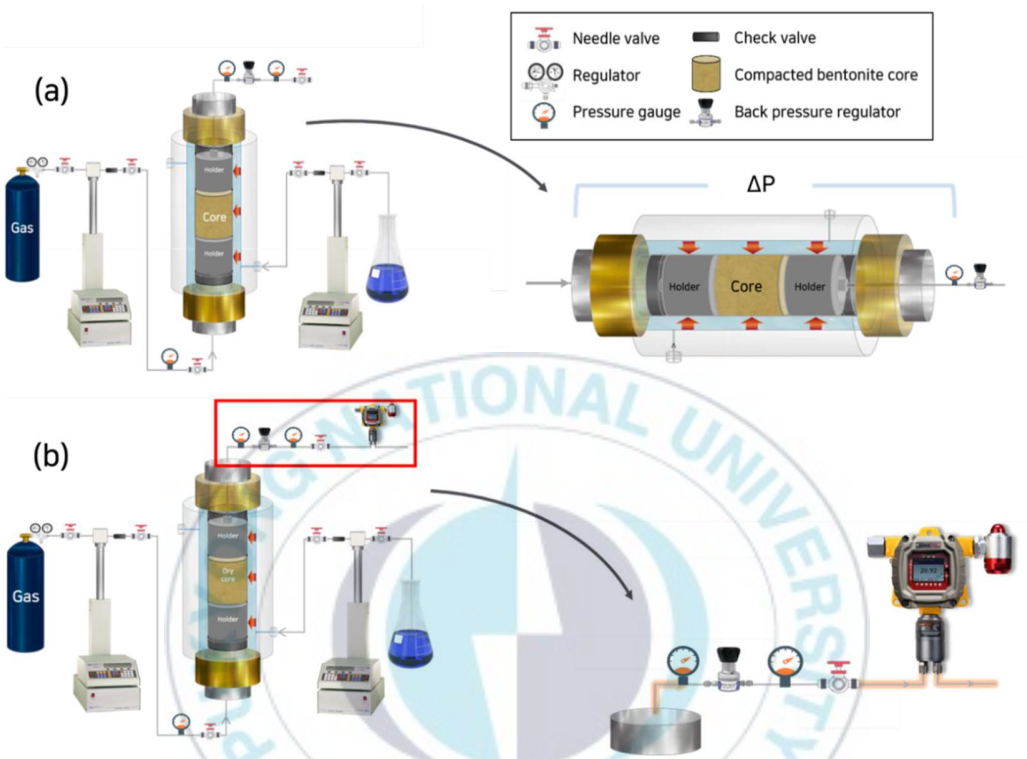

Fig. 7. Schematic of gas migration experimental apparatus.

Five factors (water content, confining pressure, injection pressure, pore pressure and dry bulk density) affecting the gas permeability and the gas migration velocity of the engineering barrier medium (the compacted WRK bentonite core) were set as variable parameter conditions for the engineering barrier in the experiment. The gas migration in the compacted WRK bentonite core was investigated by interpreting the pressure and the concentration breakthrough curves acquired from the column experiments. The effect of each influential factor on the gas migration in the barrier was evaluated and the gas flow velocity and the gas permeability for the barrier were calculated from experimental results.

The gas injection pressure on one side of the core surface was maintained higher than the pore pressure of the core, inducing the gas to flow into the core and the pressure increase or the H_2 concentration on the other side of the core was measured by the detector at certain time intervals to obtain the gas migration breakthrough curve (Figure 8). The gas permeability in the pore spaces of the core at the specific barrier condition was also calculated from the breakthrough curve and the referred parameter values at each condition.

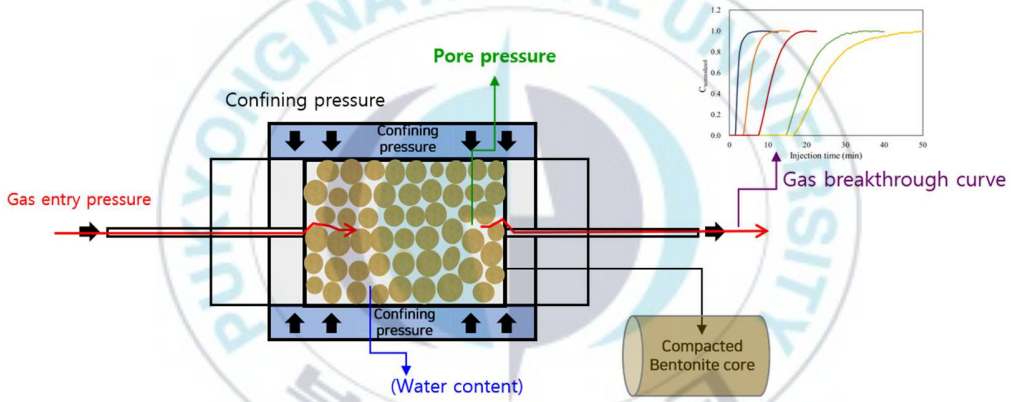

Fig. 8. Schematic of gas migration column experiment.

The pressure or the H_2 concentration breakthrough curve at the effluent of the core was normalized using the following Equation ((3) and (4)).

$$P_{normalized} = \frac{P - P_{min}}{P_{max} - P_{min}} \quad (3) \quad , \quad C_{normalized} = \frac{C - C_{min}}{P_{max} - P_{min}} \quad (4)$$

where $P_{normalized}$ is the normalized the outflow pressure, P is the outflow pressure, P_{min} is the minimum outflow pressure, P_{max} is the maximum outflow pressure, $C_{normalized}$ is the normalized of the H_2 concentration, C is the effluent H_2 concentration, C_{min} is the

minimum effluent H_2 concentration and $C_{max}$is the maximum effluent H_2 concentration.

4.4. Core experiments to find out influential parameters to control the gas migration in the barrier

The gas flow in the engineering barrier could be dependent on physical parameters such as porosity, pore size, pore pressure, pressure gradient and pore resistance as well as chemical parameters in the barrier. At the early stage of the SNF repository, the engineering barrier surrounding the Cu-canister (the compacted bentonite block) was maintained in unsaturated (or partially saturated) state because of high temperature and the early dry condition of the barrier. In this study, the gas migration into the unsaturated barrier was simulated at the different value of each physical parameter and its effect on the gas migration in the barrier was investigated through core experiments. Five main parameters including water content, pore pressure, confining pressure, injection pressure and the dry bulk density of the core were applied in core experiments. The gas migration in the compacted WRK bentonite core was applied in core experiments. The gas migration in the compacted WRK bentonite core was simulated with different values of each parameter (other parameter values were fixed) and the pressure and the H_2 concentration breakthrough curves at the outflow side of the core were acquired to estimate the average gas flow velocity and the dispersivity in the engineering barrier. The process and the result of the core experiment with different values of each parameter were described in order.

4.4.1. The effect of water content

In the early stage of the SNF repository, the engineering barrier is heated by the heat released from the Cu-canister and cooled by the inflow of groundwater. Through this heating-cooling process, the engineering barrier was slowly saturated, and an experiment was performed to simulate this. In order to perform a core experiment according to the water content, the water content of the compacted WRK bentonite core (water content: 13.1%) (provided for the experiment in KAERI) was regulated using an oven and a vacuum desiccator. The drying process was dried at 70°C for 8 hours (water content: 4.3%) and 4 hours (water content: 7.8%) using an oven, and in the addition process, 2.8g of water (water content: 14.1%) was added by putting a core in a vacuum desiccator. Core experiments with four different water contents of the core were repeated using the prepared cores and the change of the gas migrations velocity due to the water content change in the core was investigated. Detailed experimental conditions are shown in Table 3.

Table 3. Conditions for the gas migration experiment with different water content of the core.

Water content (%)				Other experimental conditions
4.3	7.8	13.1	14.1	- Gas: a gas mixed with 0.03% hydrogen and 99.97% nitrogen - Buffer medium volume: 47.69 cm^3 - Dry bulk density: 1.67 g/cm^3 - Confining pressure: 5 MPa - Pore pressure: atmospheric pressure - Pressure difference (⊿P): 0.3 MPa - Outflow pressure: 0.03 MPa - Temperature: 20℃

*⊿P: the difference between the injection pressure and the outflow pressure

4.4.2 The effect of total pore pressure

As the SNF repository goes through the evolution process, the intrusion of groundwater from the bed rock to the engineering barrier begins and the volume expansion of the compacted bentonite occurs according to the water saturation process, resulting in the porosity decrease and the pores pressure increase in the pore. The pore pressure in the barrier medium is expressed as the sum of the expansion pressure and hydrostatic pressure caused by water saturation. Although it varies depending on the depth of the repository, it is reported that it will maintain the range of 5 to 10 MPa after the middle of the disposal site evolution process (Zhang et al, 2014). But, at the early stage of the SNF repository evolution, pore spaces of the engineering barrier are empty (filled with only gas) and its pore pressure is similar to the atmospheric pressure (~ 0.1 MPa). Due to the rupture of the Cu-canister and the phase change of water by the radioactive decay heat, the gas can accumulate inside the void and the pore pressure of the barrier start to increase. As the SNF repository evolution process proceeds, these void spaces also start to be saturated with groundwater and the confining pressure around the engineering barrier also slowly increases, followed by the pore pressure increase. The gas migration in the engineering barrier will be dependent on the change of the pore pressure in the barrier. Therefore, the total pore pressure (P_t) of the compacted bentonite medium can be expressed as the sum of the hydrostatic pressure according to the repository depth (P_w), the compacted bentonite expansion pressure (P_{exe}), partial pressure (P_{vapor}) due to the vaporization of water, and the pressure raised by the confining pressure. When the gas injection pressure (P_{eg}) is greater

than the total pore pressure (P_t), the gas can move by the free phase flow as well as diffusion in the barrier medium, which is possible during the early stage of the SNF repository evolution process. Core experiments were performed to simulate the gas flow in the engineering barrier at conditions that exist at the early stage of the repository evolution (on conditions of that the barrier is dry or partially saturated and the pore pressure is different). In this study, the WRK compacted bentonite core of which pore pressure changes from 0.1 MPa (atmospheric pressure) to 7.0 MPa was used, and the average gas migration velocity in the bentonite core was measured through the breakthrough curves under specific water content and confining pressure conditions. Detailed experimental conditions are shown in Table 4.

Table 4. Conditions for the gas migration experiment with different pore pressure in the core.

Total pore pressure (MPa)					Other experimental conditions
0.3	1	3	5	7	- Gas: a gas mixed with 0.03% hydrogen and 99.97% nitrogen - Buffer medium volume: 47.69 cm^3 - Dry bulk density: 1.67 g/cm^3 - Water content: 13.05% - Confining pressure: 5 MPa - Injection pressure: 0.33, 1.3, 3.3, 5.3 and 7.3 MPa - Pressure difference (⊿P): 0.3 MPa - Outflow pressure: 0.03, 1, 3, 5 and 7 MPa - Temperature: 20℃

*⊿P: the difference between the injection pressure and the outflow pressure

4.4.3. The effect of confining pressure

At the early stage of the SNF repository, the pore pressure of the engineering

barrier and the gap pressure on the boundary of the compacted bentonite block is also similar to the atmospheric pressure (0.1 MPa), and thus the early confining pressure at the disposal hole boundary between the engineering barrier and natural barrier is not very high. However, as the SNF repository evolution proceeds, the pressure around the barrier increases up to above the hydrostatic pressure of the repository groundwater due to the inflow of bedrock groundwater around the engineering barrier and the increase of swelling pressure. This change of the confining pressure can also affect the gas migration in the barrier medium. It is considered that the higher the confining pressure, the lower the gas migration velocity to the outside of the engineering barrier because that the generated gas flow is limited in the engineering barrier, by the friction resistance and by decreasing the effective porosity. Core experiments were performed to investigate the change of the gas flow velocity in the barrier while the confining pressure ranged from 1 MPa to 20.0 MPa. Detailed experimental conditions are shown in Table 5.

Table 5. Conditions for the gas migration experiment with different confining pressure.

Confining pressure (MPa)				Other experimental conditions
1	5	10	20	- Gas: a gas mixed with 0.03% hydrogen and 99.97% nitrogen - Buffer medium volume: 47.69 cm^3 - Dry bulk density: 1.67 g/cm^3 - Water content: 13.05% - Confining pressure: 1, 5, 10 and 20 MPa - Pressure difference (⊿P): 0.3 MPa - Outflow pressure: 0.03 MPa - Temperature: 20℃

*⊿P: the difference between the injection pressure and the outflow pressure

4.4.4. The effect of injection pressure

According to previous studies, the average gas pressure generated by the radioactive decay of SNF is expected to be around 0.1 MPa. However, this gas pressure means the average gas pressure per unit area of gas generated boundary, and if the generated gas is concentrated at the specific spot on the boundary between the canister and the barrier, the injection gas pressure at that point could be much higher than the average pressure (Neretnieks and Ernstson, 1996). The gas migration velocity in the compacted WRK core was measured with various gas injection pressure conditions while the other conditions of the core were fixed. Total five different injection pressures ranged of 0.02 – 1.03 MPa were applied in the core experiment and detailed experimental conditions are shown in Table 6.

Table 6. Conditions for the gas migration experiment with different gas injection pressure.

Injection pressure (MPa)					Other experimental conditions
0.05	0.13	0.33	0.53	1.03	- Gas: a gas mixed with 0.03% hydrogen and 99.97% nitrogen - Buffer medium volume: 47.69 cm^3 - Dry bulk density: 1.67 g/cm^3 - Water content: 13.05% - Confining pressure: 5 MPa - Pressure difference (⊿P): 0.02, 0.1, 0.3, 0.5 and 1.0 MPa - Outflow pressure: 0.03 MPa - Temperature: 20℃

*⊿P: the difference between the injection pressure and the outflow pressure

4.4.5. The effect of dry bulk density

The compacted bentonite block manufactured as an engineering barrier may have a difference in gas migration according to its physical properties. The engineering barrier

should be able to prevent the gas migration in the barrier medium as much as possible by the maintaining of high pore pressure and confining pressure, originating from moderate durability, low gas permeability, and pore reduction due to the water content increase.

In this study, compacted bentonite cores having 4 different dry bulk densities were used and each gas breakthrough curve in the core was acquired to investigate the gas migration velocity change due to the different dry bulk density of the compacted bentonite block. Detailed experimental conditions are shown in Table 7.

Table 7. Conditions for the gas migration experiment with different dry bulk density of the core.

Dry bulk density (g/cm^3) (compaction load: ton)				Other experimental conditions
1.67 (0.2)	1.74 (0.4)	1.78 (0.5)	1.84 (0.6)	- Gas: a gas mixed with 0.03% hydrogen and 99.97% nitrogen - Buffer medium volume: 47.69 cm^3 - Water content: 13±0.4% - Confining pressure: 5 MPa - Injection pressure: 0.33 MPa (⊿P = 0.3 MPa) - Outflow pressure: 0.03 MPa - Temperature: 20℃

4.5. Gas permeability of bentonite core

In this study, the gas permeability of the compacted WRK bentonite core was calculated by using results from the gas migration breakthrough curve experiment. If the gas migration in the unsaturated WRK bentonite core was most dominant as the free phase flow and the gas permeability as the free phase can be obtained through Darcy's law (Equation 1). The flow of a general fluid can be obtained by using Darcy's law, but since gas has the compressibility, the volume decreases as the pressure increases. In this study,

the gas permeability of the incompressible medium through which the compressible fluid flows can be calculated through Equation 5 based on Darcy's law (Scheidegger, 1974).

$$k_{eff} = k_{ig} \cdot k_{rg} = \frac{Q_m \times \mu_g \times L \times 2P_m}{A \times (P_{in}^2 - P_{out}^2)} \quad (5)$$

Where Q_m is the total flow rate (volume of fluid as a function of time, m^3/s); A is the cross-section area of the fluid-flowing barrier medium (m^2); μ_g is the gas dynamic viscosity (Pa · s); L is the distance of the fluid barrier medium (m); and P_{in} and P_{out} are the injection pressure and the outflow pressure applied at the bottom (inlet) and the top (outlet), respectively, of the sample, and P_m is the mean pressure of P_{in} and P_{out}.

4.6. Gas flow regimes according to Knudsen number

Gas flow in a porous medium of micropore size has various flow regimes due to collision with the inner wall of the medium as well as collision between gas molecules. The gas flow regime could be divided by the value of a dimensionless parameter called the Knudsen number (Kn) (Yao et al, 2013). Knudsen number (Kn) is defined as the ratio of the molecular mean free path, λ (nm), to the average pore diameter, r (nm) (Equation 6).

$$Kn = \frac{\lambda}{r} \quad (6)$$

The gas flow regime in the compacted WRK bentonite core could be classified into four categories due to the range of the Knudsen number (Kn) (Figure 9).

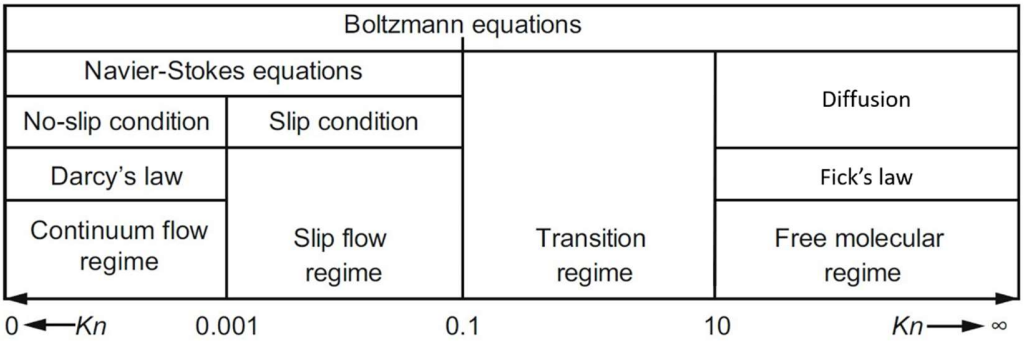

Fig. 9. Classification of the gas flow regimes and their governing equations based on the Knudsen number.

- 1) Viscous flow ($Kn < 0.01$)

If the Knudsen number (Kn) is less than 0.01, the viscous gas flow is dominant, and the Darcy's law, the existing hydrodynamic equation, can be applied for the gas migration in the core (Figure 10 (a)).

- 2) Slip flow ($0.01 < Kn < 0.1$)

A slip flow regime exists when a gas molecule slides at a solid interface. In porous media, it occurs on the wall surface within the medium. In this type of flow, the permeability obtained through the existing flow equation must be corrected by the Klinkenberg using Knudsen number (Kn) (Equation 7).

$$k_a = k_\infty(1 + 4Kn) \tag{7}$$

Where k_a is the measured gas permeability (m^2), k_∞ is the Klinkenberg's corrected permeability (m^2) and Kn is Knudsen number (Figure 10 (b)).

- 3) Transition flow ($0.1 < Kn < 10$)

Transition flow refers to the area of flow where both slip flow and diffusion flow

can occur. Existing Equations, i.e., Darcy's law with Knudsen's modification, can be applied, but there may be limitations because diffusion or slip flows dominate over viscous flows. In particular, it is more accurate to use Knudsen's diffusion equation for flows at higher Knudsen numbers (close to 10). However, in this study, since it shows a value of 2.4 or less at most of core conditions, the Klinkenberg correction using Knudsen number was applied to calculate the gas permeability of the core.

- 4) Knudsen's (free molecular) flow ($10 < Kn$)

Knudsen flows can occur under large average free paths of gas molecules, very tight voids and very low pressure condition. In petroleum engineering, it is regarded as the general flow regime of the shale gas or the methane gas formed in the coal layer.

Accordingly, the gas flow regime in the compacted WRK bentonite core could be divided into viscous flow, slip flow, transition flow, and Knudsen's flow according to the Knudsen number (Kn) (Figure 10 (c)).

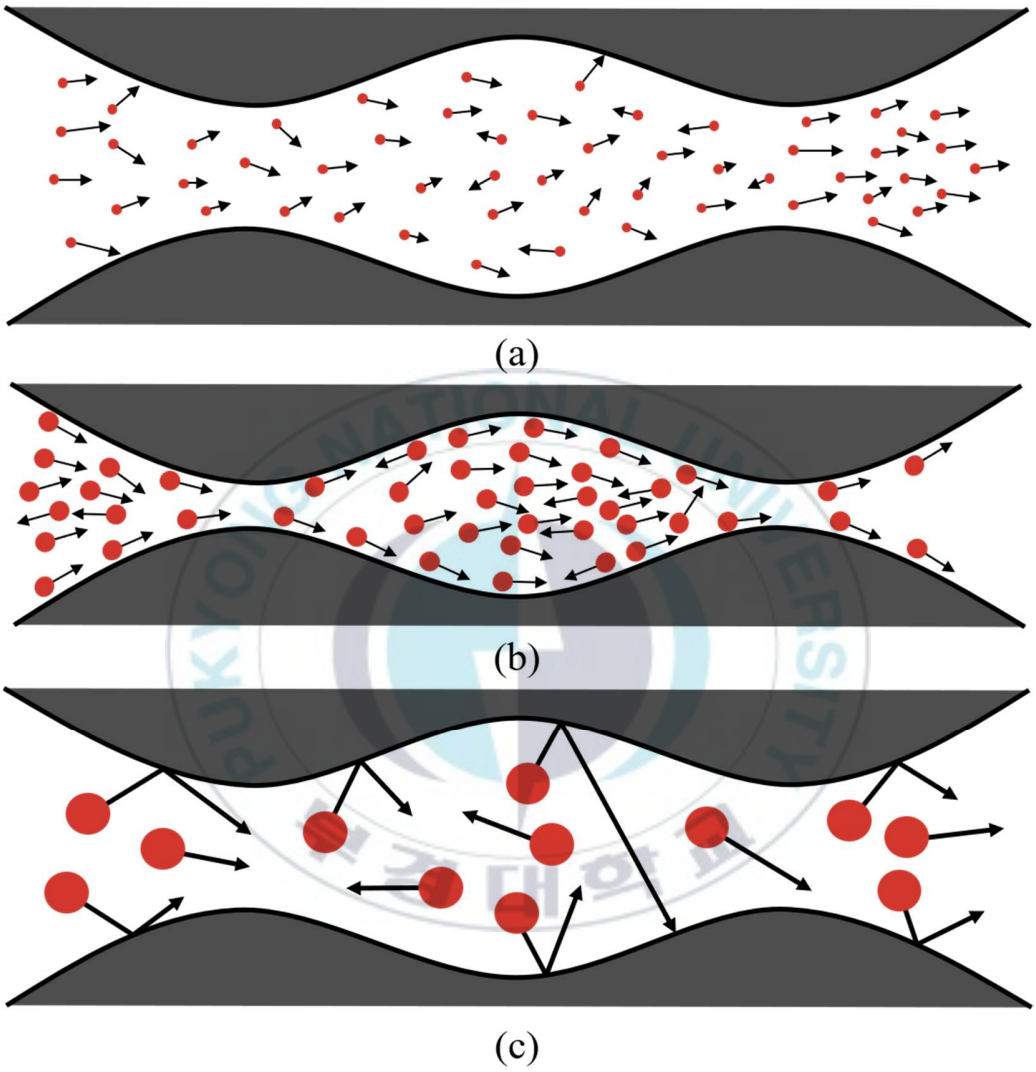

Fig. 10. Schematic of gas flow regimes according to the Knudsen number ((a) viscous flow, (b) slip flow and (c) Knudsen's flow (smaller average pore size or low pressure conditions)) (Ziarani & Aguilera, 2012).

CHAPTER 5. RESULTS AND DISCUSSION

5.1. XRD and XRF analyses

Bentonite can be classified according to the type of major cation present in montmorillonite, which is the main constituent mineral of bentonite, and the type of bentonite is classified by analyzing and comparing the contents of CaO and Na_2O in the bentonite by the XRF analysis. It is named "Ca-type bentonite" if the content of CaO is high, and "Na-type bentonite" if the content of Na_2O is high. As a result of the XRF analysis, the CaO content of the WRK bentonite was 6.52% (higher than that of the Na_2O (0.68%)) and thus, the WRK bentonite was considered to belong to the Ca-bentonite (Table 8).

Table 8. Principal composition of the WRK bentonite by the XRF result.

Component	WRK (wt%)
SIO_2	63.96
Al_2O_3	16.9
CaO	6.52
Fe_2O_3	4.94
MgO	3.98
K_2O	1.79
TiO_2	0.77
Na_2O	0.68
P_2O_5	0.22
SO_3	0.12
MnO	0.11
Total	100

Because the properties of bentonite depend on its mineral composition, the major clay minerals of the WRK bentonite was analyzed on the XRD analysis. From the results, the main constituent mineral of the WRK bentonite is montmorillonite, and other mineral is the albite, belongs to the feldspar groups, which accounts for the relatively high proportion in the bentonite (Figure 11).

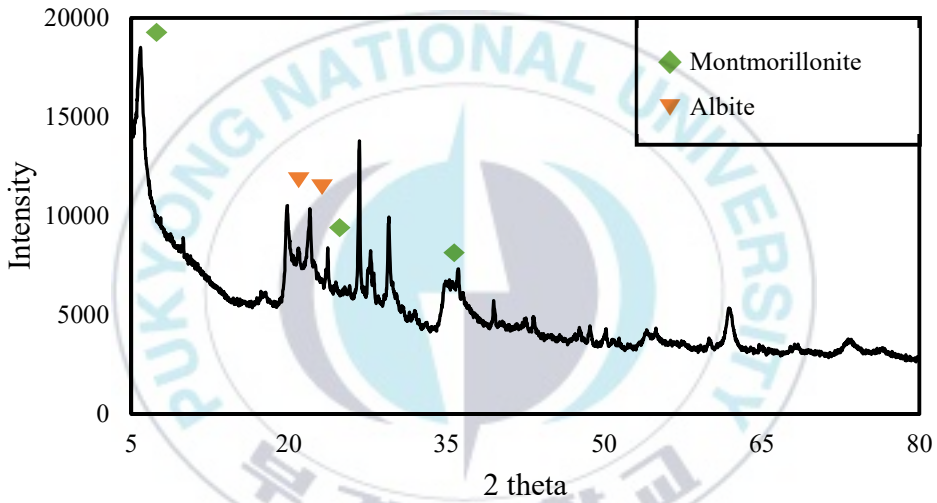

Fig. 11. Main crystalline minerals in the WRK bentonite by the XRD analysis.

5.2. Core experiments to simulate the gas migration in the engineering barrier

5.2.1. The effect of water content

The normalized pressure and the H_2 concentration breakthrough curves prepared from the experimental results with different water contents are shown in Figure 12. According to the two breakthrough curves, the velocity of the gas migration in the core was

significantly different depending on the difference in water content, but the shape of the breakthrough curve showed the typical pattern of the fluid flow by the advection in the homogeneous medium (Figure 13) (Fetter, 1999).

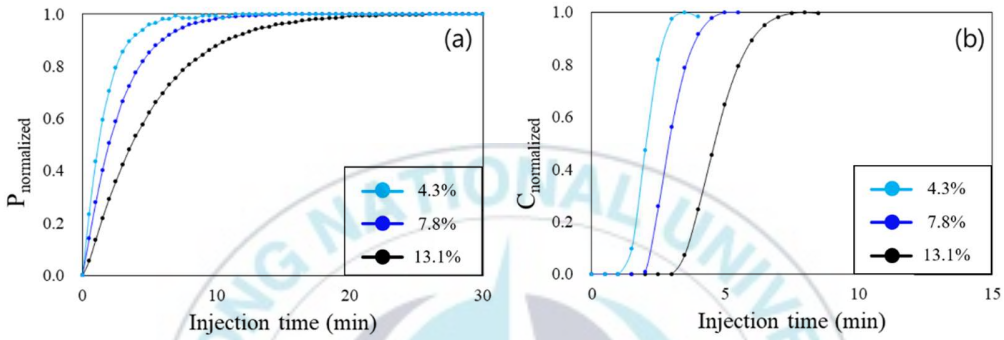

Fig. 12. Results of the gas breakthrough curve in the compacted WRK bentonite core according to the difference in water content (a: pressure breakthrough curve, b: H_2 concentration breakthrough curve).

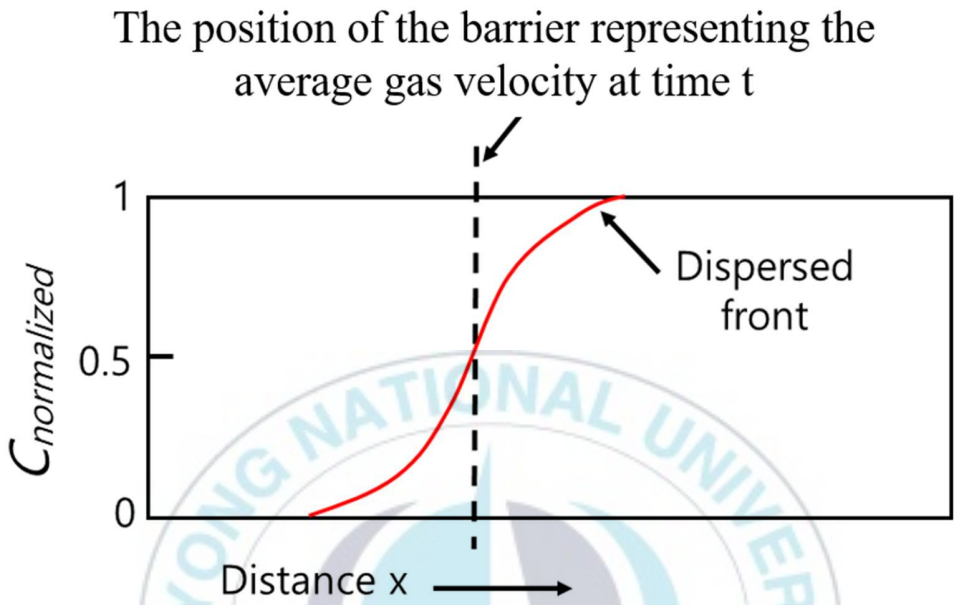

Fig. 13. Typical concentration breakthrough curve by the fluid advection and dispersion in the homogeneous medium (Fetter, 1999).

In the early stages of the repository evolution process, the engineering barrier medium is dry or unsaturated, assuming that the gas generated from the Cu-canister penetrates into the barrier due to the pressure difference between the generated gas pressure and the pore pressure. The main gas migration in the barrier medium is likely to depend on the free phase gas flow in the voids. If the gas pressure (P_g) leaked out of the canister is larger than the gas entry pressure (P_{eg}) of the medium, the inflow of gas into the barrier medium starts, and the gas in the medium migrates by the difference between the gas pressure (P_{tg}) and the total pore pressure (P_t) of the medium. Experimental result suggested that the gas generated by the rupture of the canister at the early stage of the SNF repository

can migrate quickly into the dry or partially saturated engineering barrier, and the stability of the canister and the engineering barrier must be ensured at the early stage of the SNF repository. It was found that the gas migration velocity in the barrier, of which void spaces were dry or unsaturated, was directly affected by its water content (Figure 12). The gas migration velocity by the gas phase advection in the medium decreased, but the mechanical dispersion increased as the water content of the core increased because the water phases in the pores interrupted the gas flow, causing the decrease of air route in the voids. From the H_2 concentration breakthrough curve when the water content of the core was 13.1%, the average gas migration velocity of gas in the core was about 36 cm/hour under the condition that the difference (ΔP) between gas injection pressure and pore pressure was 0.3 MPa (Figure 12). In contrast, in the case of the dried core having the water content of 4.3%, the gas migration velocity in the core increased to 90 cm/hour, 2 times faster than in the 13.1% water content core. Experimental results supported that the gas flow in dried engineering barrier can be very fast and it is very important that the multiple barrier in the SNF repository has to be appropriately constructed unless the leakage of gas from the Cu-canister and/or the gas generation in the barrier do not occur, while the engineering barrier is unsaturated in the SNF repository.

5.2.2. The effect of total pore pressure

Figure 14 shows the result of pressure breakthrough curves according to the difference in the total pore pressure in the compacted WRK bentonite core. When the pressure difference between the gas injection pressure and the pore pressure (ΔP) was

maintained at 0.3 MPa but the pore pressure in the medium was different (0.1 – 7.0 MPa), the gas migration velocity in the unsaturated compacted bentonite medium (water content: 13.1%) did not change much, but the dispersion significantly decreased as the internal pore pressure increased. In conditions that the difference (⊿P) between the injection pressure and the pore pressure is reduced from 0.3 MPa to 0.1 MPa (pore pressure: 5 MPa), the average gas migration velocity in the medium reduced by more than 2 times (about 15 cm/hour). Results suggested that the gas migration velocity in the barrier depends on the pressure difference (⊿P) between the generated gas pressure and the pore pressure rather than the pore pressure itself.

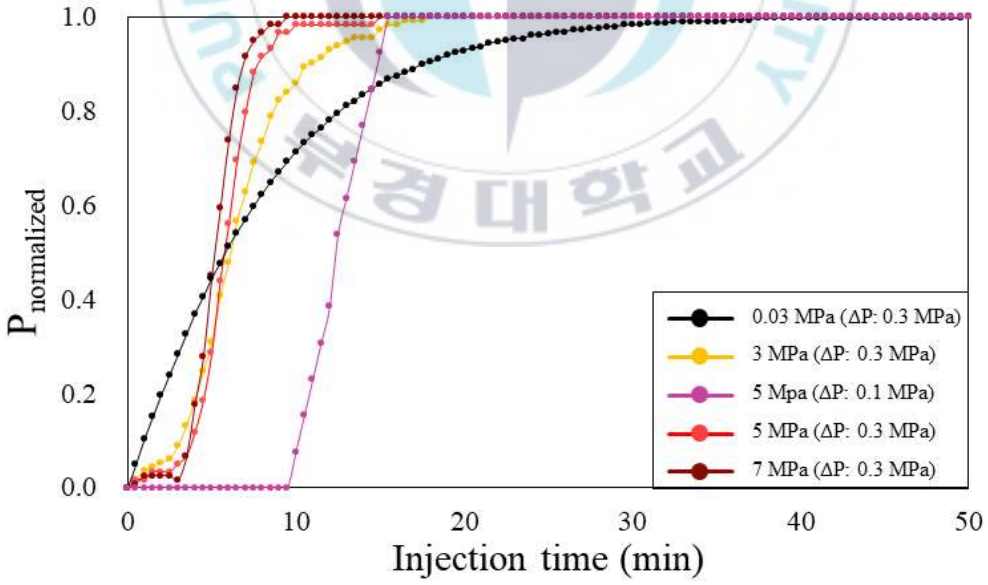

Fig. 14. Gas migration pressure breakthrough curve with various pore pressure differences (0.03 – 7 MPa) in the core.

5.2.3. The effect of confining pressure

Core experiments were performed to investigate the effect of the confining pressure on the gas migration in the engineering barrier even in the condition of the early evolution stage of the SNF repository (in unsaturated or dried engineering barrier). The pressure and the H_2 concentration breakthrough curves acquired from the experimental results are shown in Figure 15. Experimental results supported that the permeability of gas in the medium was affected by the confining pressure even when the barrier medium was dry or partially saturated, it was considered to be an effect that the internal pores in the medium were partially reduced as the confining pressure increases, and the gas in the pores is compacted by the high confining pressure in the pores, thereby increasing the frictional force between the inflow gas and the gas (or water) in the voids. In addition, the increase in confining pressure may reduce the volume of the core in proportion to the compression rate of the core, which may reduce the gas permeability due to a decrease in the volume of pores inside the compacted WRK bentonite core. At conditions of the confining pressure of 1 MPa, the injection pressure of 3.3 MPa, the water content of 13.1% in the core, and the pore pressure of the atmospheric pressure, the average migration velocity of the gas in the core was 60 cm/hour. When the confining pressure was set to 20 MPa (other conditions were the same), the average gas migration velocity in the core decreased to 9 cm/hour, supporting that the gas due to damage to the canister can migrate very fast in the barrier when the confining pressure is low at the early evolution stage also when the barrier medium is unsaturated.

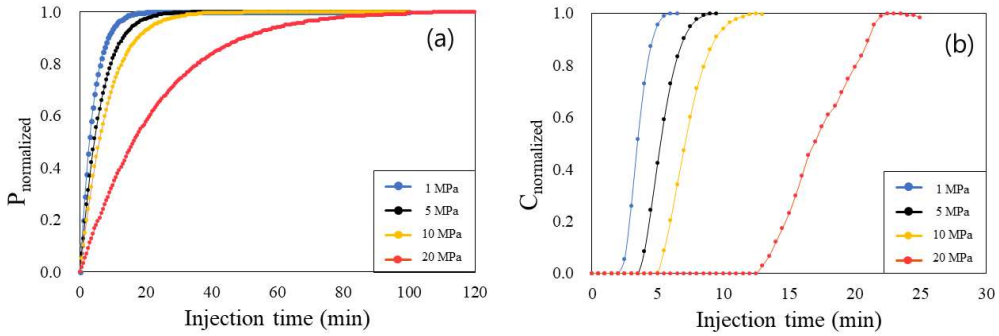

Fig. 15. Pressure breakthrough curve (a) and H_2 concentration breakthrough curve (b) in the compacted WRK bentonite core with different confining pressure (1, 5, 10 and 20 MPa).

When the confining pressure is low, the gas migration velocity in the engineering barrier is increased by cracks generated by expansion of the buffer material. In this study, it was confirmed that cracks were generated due to the expansion of the buffer when the confining pressure was not applied around the core during the process of adding water to the compacted WRK bentonite core (Figure 16). This suggests that the gas can migrate at

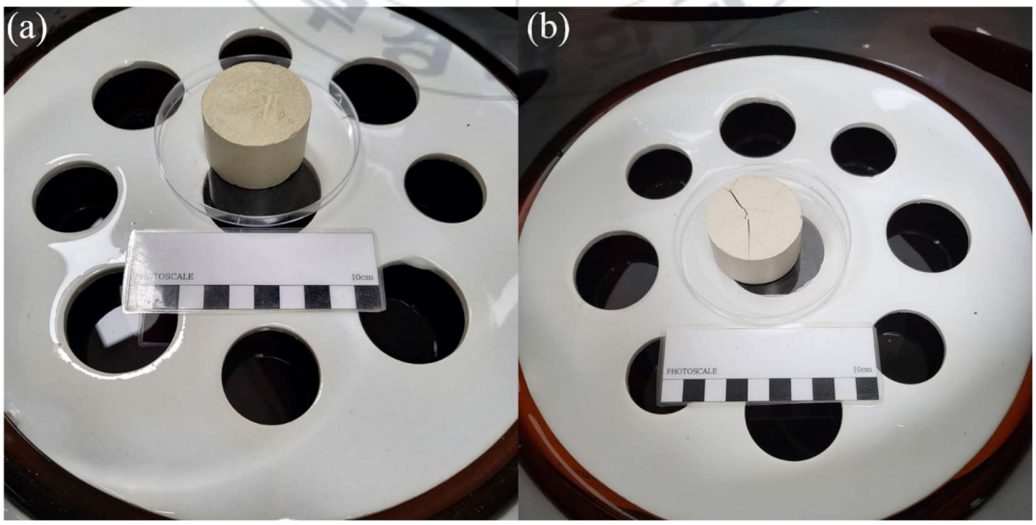

Fig. 16. Crack due to bentonite expansion due to increased water content ratio in compacted bentonite core ((a) before water supply, (b) after water supply).

a very high velocity through cracks caused by the expansion of the buffer during saturation under unsaturated conditions. The gas leakage along the barrier boundary with the low confining pressure can also happen during the early SNF repository evolution process. Therefore, it is considered very importantly to prevent the gas generation and the gas inflow into the engineering barrier at the unsaturated and the low confining pressure conditions of the engineering barrier.

5.2.4. The effect of injection pressure

The pressure breakthrough curves and the H_2 concentration breakthrough curves of gas flow in the compacted WRK bentonite core with different injection pressure were obtained from core experiments and they are shown in Figure 17. The gas flew into the unsaturated core even when the pressure difference (ΔP) between the generated gas pressure (called as "injection gas pressure" hereafter) and the pore pressure was very low (0.02 MPa) and the gas migration velocity in the core was 3.6 cm/hour. The gas migration velocity in the core increased by 10 and 25 times when the ΔP increased to 0.3 MPa and to 1.0 MPa, respectively. It was suggested that the gas can migrate into the engineering barrier at the low ΔP condition and the flow velocity was very dependent on the ΔP when the engineering barrier was unsaturated.

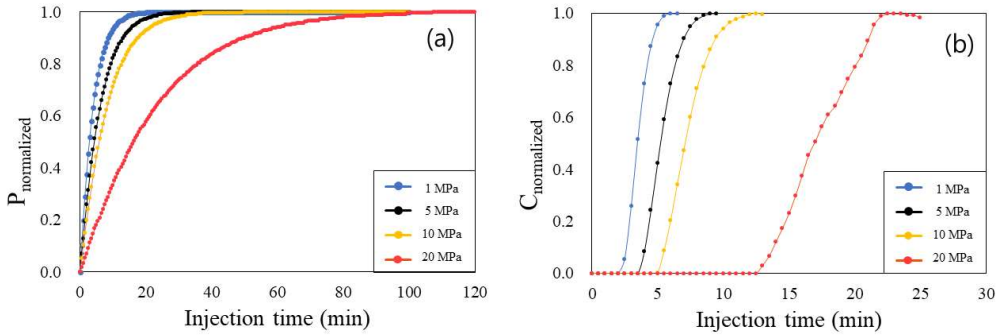

Fig. 17. Pressure breakthrough curve (a) and H_2 concentration breakthrough curve (b) with several pressure differences (ΔP: the pressure difference between the gas injection pressure and the pore pressure).

5.2.5. The effect of dry bulk density

The dry bulk density (ρ_{db}) of the compacted bentonite may affect properties of the core, resulting in the different gas migration characteristics of the core. Core experiments for the gas migration in the engineering barrier were performed with different dry bulk densities and their results are shown in Figure 18. The dry bulk density of the standard compacted WRK bentonite core is 1.67 g/cm^3, which varies depending on the load difference that is compacted during the core molding process. From experimental result, as the ρ_{db} of the core increased, the average gas migration velocity of gas in the core decreased but the degree of dispersion increased. When the ρ_{db} was 1.74 g/cm^3, the average gas migration velocity decreased by 0.2 times or more, compared to when it was 1.67 g/cm^3. When the ρ_{db} was 1.84 g/cm^3, the average gas migration velocity of the gas was reduced by more than 9 times compared to when it was 1.67 g/cm^3 (the average gas migration velocity of 3.0 cm/hour). This result is considered to be due to the decrease in the pore size through which the gas may move when the dry bulk density increases. Result suggested

that a compacted bentonite block having an appropriate drying volume density should be molded in consideration of the gas migration velocity in the medium and also be used as an engineering barrier.

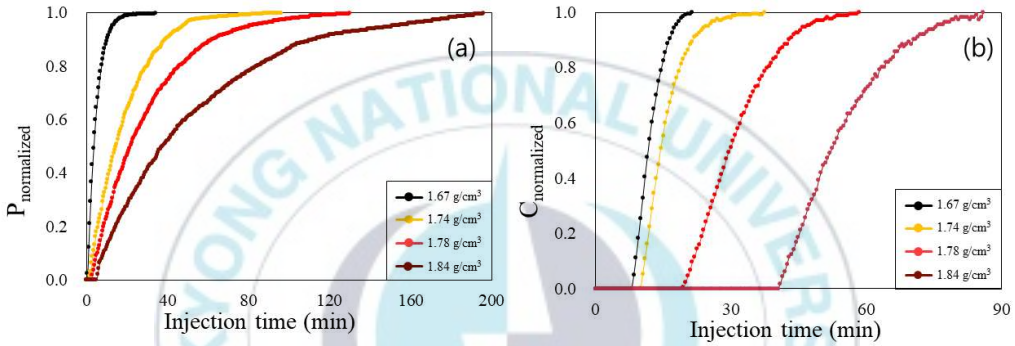

Fig. 18. Pressure breakthrough curve (a) and H_2 concentration breakthrough curve (b) with dry bulk density differences (1.67, 1.74, 1.78 and 1.84 g/cm^3).

5.3. Gas permeability of the compacted WRK bentonite core

5.3.1. The gas permeability change with various the injection pressure condition

The effective gas permeability (k_{eff}) of the compacted WRK bentonite core was calculated by using Equation (5) at various the injection gas pressure conditions. The k_{eff} was 1.17×10^{-14} m^2 at the lowest ΔP of 0.02 MPa and 1.05×10^{-15} m^2 at the highest ΔP of 1.00 MPa. As the injection gas pressure increased, the k_{eff} decreased by 11 times (Figure 19). It was inversely proportional to the injection gas pressure, the Klinkenberg effect. Therefore, the Knudsen number of each condition was applied for the Klinkenberg correction process because that the injection gas pressure conditions excluding ΔP of 0.02

MPa (Kn of 12.1) in this study belongs to a transition flow regime (0.1 < Kn < 10). The Klinkenberg correction for the k_∞ was performed by using Equation (7) and the k_{eff}, k_∞ and the average gas velovity are shown in Table 9.

Table 9. k_{eff}, k_∞ and gas velocity from the gas migration experiment and equations with different injection pressure condition.

ΔP (MPa)	0.02	0.1	0.3	0.5	1
k_{eff} ($\times 10^{-15}$ m^2)	11.71586407	3.163283	1.75738	1.405904	1.054428
k_∞ ($\times 10^{-15}$ m^2)	0.23716324	0.296188	0.414476	0.481474	0.537973
Velocity ($\times 10^{-5}$ m/s)	1.052631579	1.960784	6.666667	12.5	25
Knudsen number (Kn)	12.1	2.42	0.81	0.48	0.24
Flow regime	Knudsen's diffusion	Transition flow			

The gas permeability by the Klinkenberg correction (k_∞) was 2.96×10^{-16} m^2 at the lowest ΔP of 0.1 MPa and 5.38×10^{-16} m^2 at ΔP of 1 MPa, respectively (Figure 19). The gas permeability corrected by Knudsen number (k_∞) increased with the increase of the gas injection pressure at the constant pore pressure (ΔP increase), representing the gas velocity increase (see Figure 19). The ratio of the gas velocity to the k_∞ in the core was 7 when the injection gas pressure increased by 10 times (Figure 19). It resulted from that although the Klinkenberg correction was applied for to some extent, the correction did not completely reflect the gas flow in the core because the gas flow type was the transition flow regime rather than the slip flow regime (a regime in which the Klinkenberg correction is well fitted: 0.01 < Kn < 0.1). s the difference between the injection gas pressure, it is considered that the gas can migrate very quickly in the core of the slip flow regime.

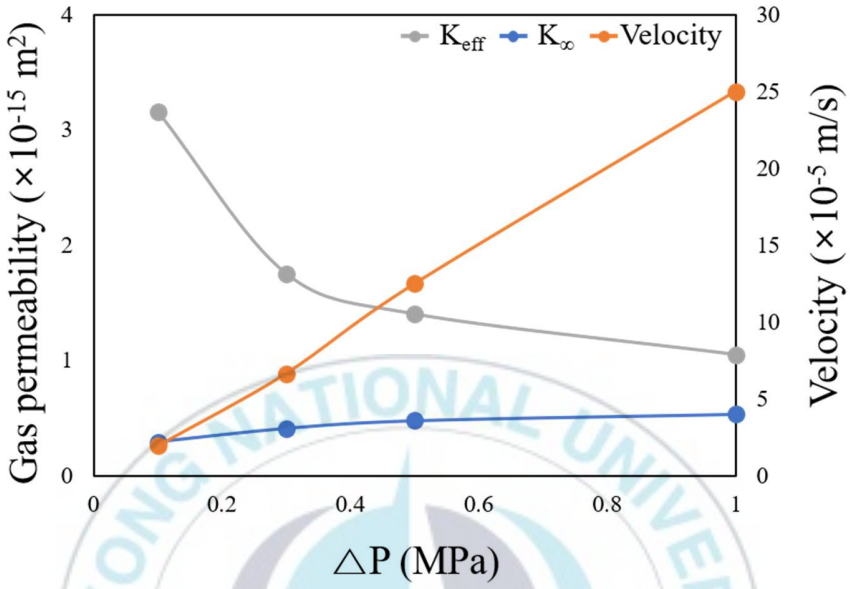

Fig. 19. Comparison of the k_{eff}, the gas permeability corrected by the Klinkenberg correction according to Knudsen number (k_{∞}) and the gas velocity under different injection pressure conditions ($\triangle P$).

5.3.2. The gas permeability of the water content condition

The k_{eff}, the modified gas permeability by the Klinkenberg correction (k_{∞}) and the average gas migration velocity with different water content are shown in Table 10. The k_{eff} is expressed as the product of the intrinsic permeability (k_{ig}) and the relative permeability (k_{rg}) (Equation 2), and the relative permeability refers to the relative ratio of two fluids in a medium (water and gas in this study). The gas migration column experiment was additionally performed to obtain the specific gas permeability with k_{rg} equal to 1 (water content of 0%). After Klinkenberg correction, the gas permeability and the gas migration velocity had similar patterns according to k_{rg}. The k_{∞} was calculated 6.72×10^{-16} m^2 at the

lowest k_{rg} of 0.29 (water content of 13.1%) and 1.79 × 10^{-15} m^2 at the k_{rg} of 0.79 (water content of 4.3%), showing a difference in permeability of 2.7 times. This difference in the gas permeability is due to a difference in a pore space in which the gas may migrate in the compacted WRK bentonite core.

Table 10. k_{eff}, k_{∞} and gas velocity from the gas migration experiment and equations with different water content conditions.

k_{rg}	1	0.7778	0.5833	0.2917
k_{eff}(× 10^{-15} m^2)	9.03795228	7.02951844	5.272139	2.636069
k_{∞} (× 10^{-15} m^2)	2.305600071	1.7932445	1.344933	0.672467
Velocity (x 10^{-5} m/s)	4.5992	3.832666667	3.193889	1.916333
Knudsen number (Kn)	0.81			
Flow regime	Transition flow			

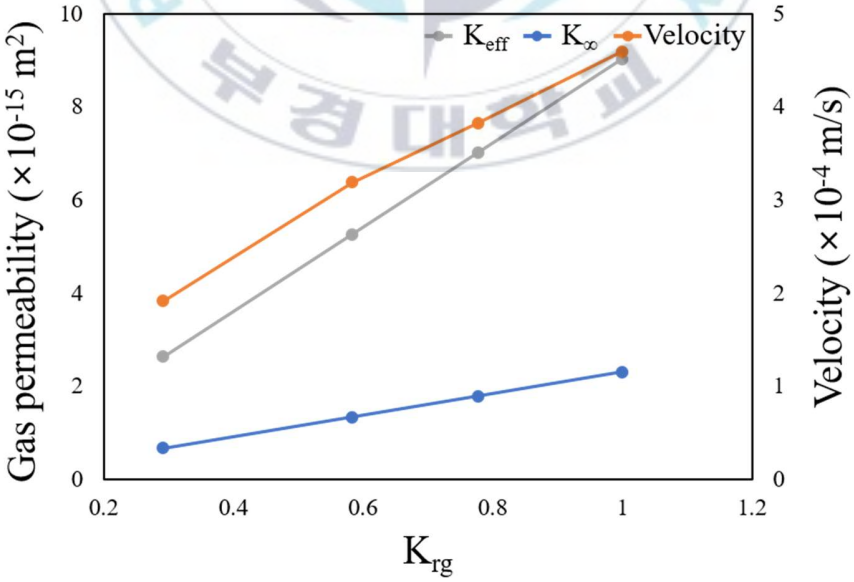

Fig. 20. Comparison of the k_{eff}, the gas permeability corrected by the Klinkenberg correction according to Knudsen number (k_{∞}) and the gas velocity under different water content conditions.

5.3.3. The gas permeability change with various confining pressure condition

Experimental results for the gas permeability at different confining pressure conditions are shown in Table 11 and Figure 21. The change of k_∞ and the gas velocity with different confining pressure conditions appeared almost the same as the confining pressure increased. The k_∞ of the core was 8.97×10^{-16} m^2 when the confining pressure was 1 MPa, and 1.63×10^{-16} m^2 at 20 MPa, showing the difference of about 5 times. It is considered that the decrease of the gas migration velocity and the gas permeability is because the confining pressure affects the gas flow regime. The gas flow regime under the confining pressure range of this study is a transition flow regime (Knudsen number is 0.81), and both of the slip flow and Knudsen's flow could occur in the core (the slip flow regime is expected to dominate). As the confining pressure of the compacted WRK bentonite core increases, the pressure on the outer wall of the core also increases, limiting the collision of gas molecules and reducing the gas migration velocity.

Table 11. k_{eff}, k_∞ and gas velocity from the gas migration experiment and equations with different confining pressure conditions.

Confining pressure (MPa)	1	5	10	20
k_{eff} ($\times 10^{-15}$ m^2)	3.51475922	2.343173	1.75738	0.639047
k_∞ ($\times 10^{-15}$ m^2)	0.89662225	0.597748	0.448311	0.163022
Velocity (x 10^{-5} m/s)	14.28571429	9.090909	6.666667	2.941176
Knudsen number (Kn)		0.81		
Flow regime		Transition flow		

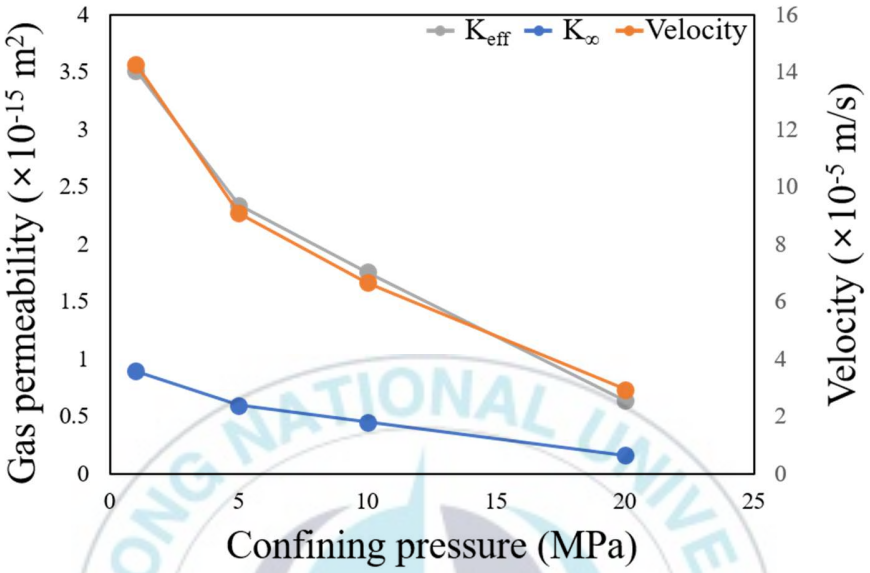

Fig. 21. Comparison of the k_{eff}, the gas permeability corrected by the Klinkenberg correction according to Knudsen number (k_{∞}) and the gas velocity under different confining pressure conditions.

5.3.4. The gas permeability change with various the dry bulk density condition

The gas permeability change according to the dry bulk density difference is shown in Table 12 and Figure 22. From the comparison of the k_{eff} with the gas migration velocity, the increase of k_{∞} and gas velocity showed the similar pattern with the bulk density change. Although the k_{∞} decreases with increasing dry bulk density, it does not completely coincide with the velocity change. The k_{∞} of the core at the lowest dry bulk density of 1.67 g/cm^3 was 6.22×10^{-16} m^2, which was 11 times larger than 5.51×10^{-17} m^2 at the highest dry bulk density of 1.84 g/cm^3. This difference in the k_{∞} and the gas velocity was considered to be due to the decrease in porosity and the size of pores according to the compression load (0.2~0.4 ton) during the manufacturing process of the compacted WRK bentonite core

(Table 2). Therefore, the change in the k_∞ and the gas migration velocity according to dry bulk density change is considered that the gas flow regime in the core is changed by the difference in the average pore size. Through the calculated Knudsen number, it is considered that all four samples belong to the transition flow regime, but the k_∞ of the core in which the Knudsen's flow was more dominant, was reduced due to the difference in Knudsen number.

Table 12. k_{eff}, k_∞ and gas velocity from the gas migration experiment and equations with different dry bulk density conditions.

Dry bulk density (g/cm^3)	1.67	1.74	1.78	1.84
K_{eff} ($\times 10^{-15}$ m^2)	2.636069415	0.781058	0.490432	0.288884
K_∞ ($\times 10^{-15}$ m^2)	0.621714485	0.165478	0.095787	0.055131
Velocity (x 10^{-5} m/s)	9.090909091	3.448276	1.666667	0.952381
Knudsen number (Kn)	0.81	0.93	1.03	1.06
Flow regime	Transition flow			

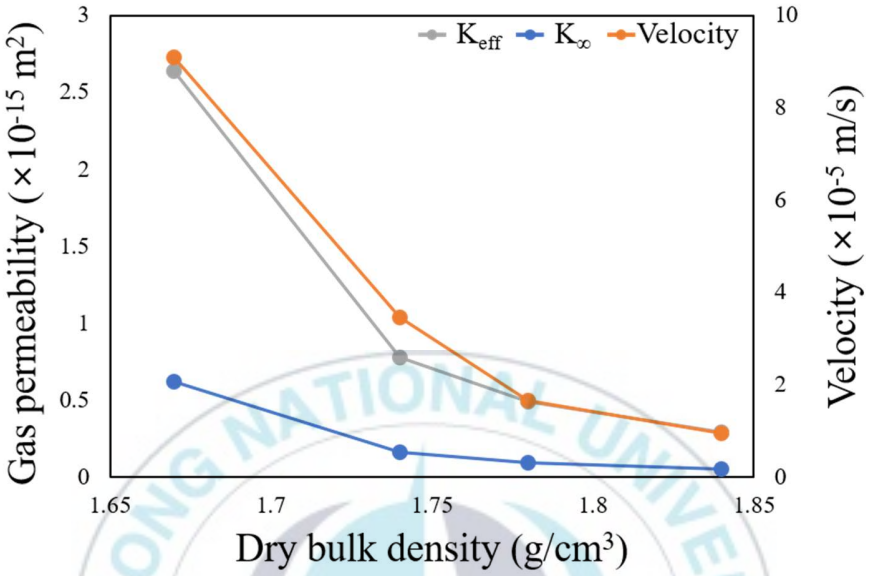

Fig. 22. Comparison of the k_{eff}, the gas permeability corrected by the Klinkenberg correction according to Knudsen number (k_{∞}) and the gas velocity under different dry bulk density conditions.

CHAPTER 6. CONCLUSIONS

This study focused on the investigation of the gas migration characteristics in the engineering barrier at the early stages during the SNF repository evolution process. Gas migration experiments in the compacted WRK bentonite selected as the engineering barrier materials in the Korean SNF repository were performed. The average gas velocity in the compacted bentonite core was calculated by using the breakthrough curves acquired from the laboratory scale experiments at different conditions of five main parameters, controlling properties of the gas migration in the porous medium (the injection pressure, the pore pressure, the water content, the confining pressure and the dry bulk density). The effective gas permeability (k_{eff}) of the compacted WRK bentonite core based on experimental results was also calculated and they were compared to each other at different conditions of each parameter, determining the main effective factor for the gas flow velocity in the core. The modified gas permeability (k_{∞}) was obtained by the Klinkenberg correction process to experimental results in order to exactly represent the gas migration in the core. From these results, the gas migration in the pore spaces of the compacted WRK bentonite core was divided into several gas flow regimes, explaining the main gas flow mechanisms.

From the experimental results, the average gas migration velocity and the gas permeability in the compacted WRK bentonite core at the unsaturated condition were calculated. The gas migrated in the compacted WRK bentonite core at an average rate of 3.0~90 cm/hour, and its gas permeability ranged from 2.31×10^{-15} m^2 to 5.51×10^{-17} m^2.

Results supported that at the unsaturated barrier conditions of the SNF repository, the gas will migrate in the engineering barrier at a very high velocity and in the form of the diffusion and/or the slip flow as well as the viscous flow (the transition flow regime: $0.1 < Kn$ (Knudsen number) < 10). Therefore, it is essential to develop techniques securing the stability of engineering barriers and the Cu-canisters to prevent leakage by minimizing gas generation and migration. Results from this study would serve to understand quantitatively the gas migration mechanism in the engineering barrier and to extend the gas-nuclide conjugated migration study at the saturated condition.

REFERENCES

"bentonite". (2021) Lexico UK English Dictionary. Oxford University Press. Archived from the original on April 27.

Ahn, J., Kim, W. S., Park, J. B., Francis, A. J. & Um, W. (2019). Temporal changes of geochemistry and microbial community in low and intermediate level waste (LILW) repository, South Korea. Annals of Nuclear Energy, 128, 309-317.

An, R., Yu, B., Li, R. & Wei, Y. M. (2018). Potential of energy savings and CO2 emission reduction in China's iron and steel industry. Applied Energy, 226, 862-880.

Bond, A. E., Hoch, A. R., Jones, G. D., Tomczyk, A. J., Wiggin, R. M. & Worraker, W. J. (1997). Assessment of a spent fuel disposal canister. Assessment studies for a copper canister with cast steel inner component. Sweden.

Choung, S., Um, W., Choi, S., Francis, A. J., Kim, S., beak Park, J. & Kim, S. H. (2014). Biogeochemical changes at early stage after the closure of radioactive waste geological repository in South Korea. Annals of Nuclear Energy, 71, 6-10.

Cuss, R., Harrington, J., Giot, R. & Auvray, C. (2014). Experimental observations of mechanical dilation at the onset of gas flow in Callovo-Oxfordian claystone. Geological Society, London, Special Publications, 400(1), 507-519.

Davis, R. O. & Selvadurai, A. P. (2005). *Plasticity and geomechanics*. Cambridge

university press.

Fetter, C. W., Boving, T. B. & Kreamer, D. K. (1999). *Contaminant hydrogeology* (Vol. 500). Upper Saddle River, NJ: Prentice hall.

Hamilton, L. H., Scowcroft, B., Ayers, M. H., Bailey, V. A., Carnesale, A., Domenici, P. V. & Sharp, P. (2012). Blue Ribbon Commission on America's Nuclear Future: Report to the Secretary of Energy. Blue Ribbon Commission on America's Nuclear Future (BRC), Washington, DC.

Hebel, L. C., Christensen, E. L., Donath, F. A., Falconer, W. E., Lidofsky, L. J., Moniz, E. J. & APS Council Review Committee. (1978). Report to the American Physical Society by the study group on nuclear fuel cycles and waste management. Reviews of Modern Physics, 50(1), S1.

Hoch, A. R., Cliffe, K. A., Swift, B. T. & Rodwell, W. R. (2004). Modelling gas migration in compacted bentonite: gambit club phase 3. Final report (No. POSIVA--04-02). Posiva Oy.

Horseman, S. T., Harrington, J. F. & Sellin, P. (1999). Gas migration in clay barriers. Engineering Geology, 54(1-2), 139-149.

IAEA. (2022). In operation & suspended operation. https://pris.iaea.org/PRIS/WorldStatistics/OperationalReactorsByCountry.aspx

Karnland, O. (2010). *Chemical and mineralogical characterization of the bentonite buffer for the acceptance control procedure in a KBS-3 repository*. Sweden.

Kim, J., Kim, J., Jung, H. & Ha, J. C. (2013). Experiment on gas entry pressure and gas permeability of concrete silo for a low-and intermediate-level waste disposal facility in Korea. Nuclear Engineering and Design, 265, 841-845.

Kim, J., Kim, S., Park, J. B. & Lee, S. (2010a). Planning of large-scale in-situ gas generation experiment in Korean Radioactive Waste Repository. In International Conference on Radioactive Waste Management and Environmental Remediation (Vol. 54525, pp. 27-31).

Kim, K. I., Lee, C. & Kim, J. S. (2021). A numerical study of the performance assessment of coupled thermo-hydro-mechanical (THM) processes in improved korean reference disposal system (kRS+) for high-level radioactive waste. Tunnel and Underground Space, 31(4), 221-242.

Kim, S. H., Kim, J. Y., Park, J. B. & Lee, S. J. (2010b). Preliminary evaluation of gas generation from the Korean LILW Repository using the SMOGG Code. In Transaction of the Korean Nuclear Society Autumn Meeting, Jeju.

Kim, T., Lee, C., Kim, J. W., Kang, S., Kwon, S., Kim, K. I. & Kim, J. S. (2021). Introduction to Tasks in the International Cooperation Project, DECOVALEX-2023 for the Simulation of Coupled Thermohydro-mechanical-chemical Behavior in a Deep Geological Disposal of High-level Radioactive Waste. Tunnel and Underground Space, 31(3), 167-183.

King, F. & LeNeveu, D. (1992). Prediction of the lifetimes of copper nuclear waste containers. In Proceedings of Conference on Nuclear Waste Packaging, FOCUS

(Vol. 91, pp. 253-261).

King, F., Kolář, M., Puigdomenech, I., Pitkänen, P. & Lilja, C. (2021). Modeling microbial sulfate reduction and the consequences for corrosion of copper canisters. Materials and Corrosion, 72(1-2), 339-347.

King, F., Kolar, M., Vähänen, M. & Lilja, C. (2011). Modelling long term corrosion behaviour of copper canisters in KBS-3 repository. Corrosion Engineering, Science and Technology, 46(2), 217-222.

King, F., Lilja, C. & Vähänen, M. (2013). Progress in the understanding of the long-term corrosion behaviour of copper canisters. Journal of Nuclear Materials, 438(1-3), 228-237.

Klinkenberg, L. J. (1941). The permeability of porous media to liquids and gases. Am. Petrol. Inst., Drilling and Production Practice, 2, 200-213.

Knudsen, M. (1909). Die Gesetze der Molekularströmung und der inneren Reibungsströmung der Gase durch Röhren. Annalen der Physik, 333(1), 75-130.

Kohno, M., Nara, Y., Kato, M., & Nishimura, T. (2018). Effects of clay-mineral type and content on the hydraulic conductivity of bentonite–sand mixtures made of Kunigel bentonite from JapanMasanori Kohno et al. Effects of clay mineral type and content on hydraulic conductivity. Clay Minerals, 53(4), 721-732.

Kwon, S. K. & Cho, W. J. (2011). Reviews on investigation of high-level nuclear wastes and studies on rock mechanics of underground disposal research facilities. In

Conference Proceeding of The Korean Society for Rock Mechanics, pp. 111-120.

Lee, C. (2013). External Costs of Nuclear Energy in Korea. A Study on Climate and Environmental Policy, 534-684.

Lee, C. Y., Jang, W. Y., Jeon, Y. H., Lee, J. Y. & Lee, K. K. (2000). A Study on Air Permeability and Radius of Influence During SVE/Bioventing. Journal of Korean Society of Groundwater Environment, 7(1), p24-31.

Lee, C., Yoon, S., Cho, W. J., Jo, Y., Lee, S., Jeon, S. & Kim, G. Y. (2019). Study on thermal, hydraulic, and mechanical properties of KURT granite and Gyeongju bentonite. Journal of Nuclear Fuel Cycle and Waste Technology, 17, 65-80.

Lee, J. J. (2006). Current Status and Future Prospects of Nuclear Power Generation in Korea. Nuclear Industry, 26(4), 22-25.

Lee, J. O. & Cho, W. J. (2007). Thermal-Hydro-Mechanical Behaviors in the Engineered Barrier of a HLW Repository: Engineering-scale Validation Test. Tunnel and underground space, 17(6), 464-474.

Lee, J., Cho, D., Choi, H. & Choi, J. (2007). Concept of a Korean reference disposal system for spent fuels. Journal of Nuclear Science and Technology, 44(12), 1565-1573.

Li, C., Xu, P., Qiu, S., & Zhou, Y. (2016). The gas effective permeability of porous media with Klinkenberg effect. Journal of Natural Gas Science and Engineering, 34, 534-540.

Marschall, P., Horseman, S. & Gimmi, T. (2005). Characterisation of gas transport

properties of the Opalinus Clay, a potential host rock formation for radioactive waste disposal. Oil & Gas Science and Technology, 60(1), 121-139.

Maxwell, J. C. (1879). On stresses in rarefied gases arising from inequalities of temperature The Scientific Papers of James Clerk Maxwell.

McCollom, T. M., Klein, F., Robbins, M., Moskowitz, B., Berquó, T. S., Jöns, N., Bach, W. & Templeton, A. (2016). Temperature trends for reaction rates, hydrogen generation, and partitioning of iron during experimental serpentinization of olivine. Geochimica et Cosmochimica Acta, 181, 175-200.

Muyzer, G. & Stams, A. J. (2008). The ecology and biotechnology of sulphate-reducing bacteria. Nature Reviews Microbiology, 6(6), 441-454.

N.R.C. (2001a). Disposition of high-level waste and spent nuclear fuel. Committee on Disposition of High-Level Radioactive Waste through Geological Isolation. Board of Radioactive Waste Management, 22-26.

N.R.C. (2001b). Disposition of high-level waste and spent nuclear fuel: the continuing societal and technical challenges. National Academies Press.

N.R.C. (2012). High-Level Waste. Rockville, MD: US NRC. http://www.nrc.gov/waste/high-level-waste.html

Nash, P. J., Swift, B. T., Goodfield, M. & Rodwell, W. R. (1998). Modelling gas migration in compacted bentonite. A report produced for the GAMBIT club (No. POSIVA--98-08). Posiva Oy.

Neretnieks, I. & Ernstson, M. L. (1996). A note on radionuclide transport by gas bubbles. MRS Online Proceedings Library (OPL), 465.

North, D. W. (1997). Unresolved problems of radioactive waste: Motivation for a... Physics Today, 50(6), 48-54.

NWMO. (2005). Choosing a Way Forward; The Future Management of Canada's Used Nuclear Fuel—Final Study Summary.

Park, J. B., Lee, S. J., Kim, S. H. & Kim, J. Y. (2010). Analysis of case studies on experimental research of gas generation in foreign countries for low-and intermediate-level radioactive waste disposal. Journal of Nuclear Fuel Cycle and Waste Technology (JNFCWT), 8(3), 229-238.

Pitkänen, P. & Partamies, S. (2007). Origin and Implications of Dissolved Gases in Groundwater at Olkiluoto. Posiva report 2007-04, Posiva Oy, Olkiluoto. Available online at: http://www.posiva.fi/files/341/Posiva2007-04web.pdf

Ritchie, H. 2020. Emissions by Sector. Our World in Data. Available online: https://ourworldindata.org/emissions-by-sector (accessed on 24 November 2022)

Sellin P. (ed.) 2014. Experiments and Modelling on the behaviour of EBS. FORGE Reprot, D3.38. :s.n, s.l.

Sellin, P. & Leupin, O. X. (2013). The use of clay as an engineered barrier in radioactive-waste management–a review. Clays and Clay Minerals, 61(6), 477-498.

Shaw, R. P. (Ed.). (2015). Gas generation and migration in deep geological radioactive

waste repositories. Geological Society of London.

Thauer, R. K., Jungermann, K. & Decker, K. (1977). Energy conservation in chemotrophic anaerobic bacteria. Bacteriological Reviews, 41(1), 100-180.

Villar, M. V., Gutierrez-Rodrigo, V., Martín, P. L., Romero, F. J. & Barcala, J. M. (2014). Gas transport in bentonite. Technical Report of CIEMAT, ISSN (2014), pp. 1135-9240

Wada, Y., Kawaguchi, K. & Myouchin, M. (1995). Decomposition of water and production of H2 using semiconductor-photocatalytic effect induced by gamma ray from high radioactive waste. Progress in Nuclear Energy, 29, 251-256.

Wersin, P., Spahiu, K. & Bruno, J. (1994). Kinetic modelling of bentonite-canister interaction. Long-term predictions of copper canister corrosion under oxic and anoxic conditions (No. SKB-TR--94-25). Swedish Nuclear Fuel and Waste Management Co.

Whiticar, M. J. (1999). Carbon and hydrogen isotope systematics of bacterial formation and oxidation of methane. Chemical Geology, 161(1-3), 291-314.

Wikramaratna, R. S., Goodfield, M., Rodwell, W. R., Nash, P. J. & Agg, P. J. (1993). A preliminary assessment of gas migration from the copper/steel canister (No. SKB-TR--93-31). Swedish Nuclear Fuel and Waste Management Co.

Wilson, J. (2017). FEBEX-DP: Geochemical Modelling of Iron-Bentonite Interactions. Quintessa's Contribution on Behalf of RWM QRS-1713A-R3, 1.3.; Quintessa

Limited: Oxford, UK, 2017; p. 68.

Yao, J., Sun, H., Fan, D. Y., Wang, C. C. & Sun, Z. X. (2013). Numerical simulation of gas transport mechanisms in tight shale gas reservoirs. Petroleum Science, 10(4), 528-537.

Zhang, M., Zhang, H., Zhou, L., Wang, B. & Wang, S. (2014). Hydro-mechanical analysis of GMZ bentonite–sand mixtures in the water infiltration process as the buffer/backfill mixture in an engineered nuclear barrier. Applied Clay Science, 97, 115-124.

Ziarani, A. S. & Aguilera, R. (2012). Knudsen's permeability correction for tight porous media. Transport in Porous Media, 91(1), 239-260.

국내 사용후 핵연료 처분장 초기 진화 과정 동안 공학적 방벽 내에서의 가스 거동 특성 규명

김 단 우

부경대학교 대학원 지구환경시스템과학부

지구환경과학전공

요약문

지질학적 심층 처분은 사용후 핵연료(SNF)를 영구적으로 격리하는 가장 효과적인 방법 중 하나로 연구되고 있다. 많은 원자력발전소의 사용과 그에 따른 임시저장시설의 포화로 인해 SNF를 영구적으로 폐기하기 위한 처분장의 건설과 관련 연구 및 기술개발이 매우 시급한 실정이다. 지질학적 심층 처분은 방사성 핵종이 생물권으로 유출되는 것을 방지할 수 있는 자연장벽과 공학장벽으로 설계된 다중장벽시스템에 SNF가 보관된 구리저장용기를 반영구적으로 매설하는 처분 방법이다. SNF가 처분장에 처분된 후 SNF의 연속적인 핵분열과 구리 저장용기 및 다중 방벽에서의 지구화학적, 생물학적 반응으로 가스가 생성될 수 있다. 생성된 가스의 이동은 다중 방벽 내 핵종 이동에 영향을 미칠 수 있으며 최종적으로 처분장 부지의 안전에 영향을 미칠 수 있다. 본 연구에서는 SNF 처분장의 지질학적 진화 초기 단계에서 불포화 상태인 공학적 방벽 내의 가스 거동을 모사하기 위해 실험실 규모의 실험을 수행하였다. 혼합가스(0.03% H_2 + 99.97% N_2)와 압축 WRK 벤토나이트 코어(건조 용적 밀도 1.67 g/cm3, 직경 4.5 cm, 높이 3 cm)를 실험에 사용하였다. 실험에 앞서 SNF 처분장 진화 과정 초기 단계의 공학적 방벽 내 가스 이동에 영향을 미치는 5가지 매개변수(주입 가스 압력, 수분 함량, 주변압, 건조 용적 밀도 및 총 공극 압력)를 설정하였고, 가스 거동을 시뮬레이션하기 위해 칼럼 실험을 수행했다. 실험을 통해 압축 WRK 벤토나이트 코어의 각 매개변수에 대한 가스상에서의 압력 돌파 곡선과 H_2 농도 돌파 곡선을 얻었다. 코어 내 평균 이동속도는

파과곡선을 통해 얻은 데이터를 이용하여 계산하였으며, 특정 코어 조건에서의 유효 가스 투과도는 Klinkenberg 보정을 통해 다공성 매질 내 가스 미끄러짐 효과를 고려하여 계산하였다.

압축 WRK 벤토나이트 코어 내 주입 가스 압력은 SNF 처분장의 공학적 방벽 내부의 가스 발생 및 유입을 의미한다. 본 연구에서는 공학적 방벽 경계에서의 주입압이 방벽 매질의 공극압보다 높아지면 가스가 코어로 이동하여 SNF 처분장을 내에서 분산될 수 있다. 주입 가스 압력 조건은 △P(주입압과 코어 내 총 공극압의 압력 차이)를 0.02, 0.1, 0.3, 0.5, 1.0 MPa로 설정하여 적용하였다. 압축 WRK 벤토나이트 코어의 평균 가스 이동 속도는 주입압이 50배 증가하였을 때 25배 증가하였다. 주입압과 공극압을 이용하여 계산한 k_{eff}는 압력차($\triangle P$)의 역에 비례하는 전형적인 Klilnkenberg 효과를 나타내었다. Klinkenberg 보정(k_∞)에 의해 보정된 가스 투과도는 주입 가스 압력이 10배 증가하였을 때 1.8배 증가하였다. 압력은 투과성에 대한 속도의 비율에 비례하지만, 본 연구에서는 압력이 10배 증가하였을 때 투과성에 대한 속도의 비율이 7배 증가하였다. 이러한 차이는 Klinkenberg 보정이 전이 흐름 체제에서는 완전히 보정되지 않기 때문이다.

수분 함량은 SNF 처분장의 공학적 방벽에서 공극을 제어하는 매개 변수이다. 컬럼 실험은 수분 함량 4.3%, 7.8%, 13.1% 조건에서 수행되었다. 코어 내 수분 함량이 13.1%에서 4.3%로 증가함에 따라 가스 이동 속도와 보정된 가스 투과도(k_∞)가 각각 2배, 2.7배 증가하였다. 완충기 내 수분 함량의 감소는 공극 공간을 증가시키고 가스 이동 속도를 증가시키기 때문이다. 수분함량에 따른 실험의 결과를 통해 SNF 처분장의 초기 진화 동안 Cu 보관용기에서 방출된 열로 인해 공학적 방벽이 건조할 때 가스가 매우 빠르게 공학적 방벽으로 이동할 수 있다는 것을 뒷받침한다(시간당 36~72cm).

주변압은 공학적 방벽 완충재의 외벽에 가해지는 압력으로, 대기압에서부터 SNF 처분장의 깊이에 따른 정수압 이상의 높은 압력으로 점점 증가한다. 본 연구에서는 1, 5, 10, 20 MPa의 주변압 조건에서 평균 가스 이동 속도와 k_∞를 계산하였다. 실험의 획기적인 곡선에서 평균 가스 이동 속도는 주변압이 20배 감소함에 따라 약 6.7배 더 빨라지고 k_∞는 6배 더 증가했다. 주변압 감소에 의한 평균 가스 이동 속도와 k_∞의 증가는 거의 동일한 것으로 나타났다.

건조 용적 밀도는 압축 WRK 벤토나이트 코어(공학적 방벽의 완충재)의 물리적 특성 중 하나로, 내구성, k_∞, 공학적 방벽의 팽창 압력에 영향을 미친다. 가스 거동 실험에는 1.67, 1.74, 1.78, 1.84 g/cm^{3}의 4가지 다른 건조 용적 밀도를 갖는 코어가 사용되었다. 건조 용적 밀

도가 1.67 g/cm^{3}에서 1.84 g/cm^{3}로 증가함에 따라 건조 용적 밀도에 따른 평균 가스 거동 속도가 약 9.5배(3.4 cm/hour에서 32.7 cm/hour로) 감소하였다. 또한 k_∞는 건조 용적 밀도가 증가함에 따라 약 11배(5.51 × 10-17에서 6.22 × 10-16 m2로) 감소했다. 그러나 평균 가스 거동 속도에 대한 k_∞의 비율은 용적 밀도 감소와 일치하지 않았다. 이는 평균 공극 크기의 감소에 따른 코어의 가스 흐름 체제의 차이 때문이다.

코어 내의 총 공극압은 정수압, 벤토나이트 완충재의 팽창압 및 수증기화에 의해 증가된 부분압의 합이다. 본 실험에서는 주입 가스 압력이 0.53, 1.03, 3.03, 5.03, 7.03 MPa로 차이가 나지만, $\triangle P$는 0.3 MPa (공극압: 0.50, 1.00, 3.00, 5.00, 7.00 MPa)로 유지되었다. 코어 내 가스의 파과곡선으로부터 공극압차에 의한 가스이동속도의 차이는 매우 적었으나, 코어 내의 공극압이 증가할수록 코어 내 가스분산도가 뚜렷하게 감소하였다. 즉, 불포화 공학적 방벽 내에서 공극 압력이 높더라도 $\triangle P$가 일정하면 동일한 속도로 가스가 이동하는 것을 의미한다.

수행된 실험들의 결과를 통해, 불포화 조건에서의 압축 WRK 벤토나이트 코어에 대한 평균 가스 거동 속도와 Klinkenberg 효과로 보정된 가스 투과도(k_∞)는 각각 3.0~90.0 cm/hour , 2.31 × 10^{-15} m2~5.51 × 10^{-17} m2 였다. 따라서 본 연구를 통해 SNF 처분장 진화 과정 초기에는 불포화 상태인 공학적 방벽에서 매우 빠른 속도로 가스가 이동한다는 것을 시사하였으며, SNF 처분 초기에는 가스 거동이 빨라 Cu 보관용기와 공학적 방벽의 안전성에 대해 기술적으로 제어할 방법을 마련하는 것이 중요하다.

주제어: 사용후 핵연료 처분장, 가스 생성, 가스 거동, 공학적 방벽, 가스 투과성, 클린켄베르그 효과, 크누센 수

감사의 글

2012년 입학 이후 다사다난한 20대를 겪고 10년만에 드디어 졸업하게 되었습니다. 우선 Lee family의 일원이 되게 해주신 이민희 교수님께 진심으로 감사드립니다. 실험실 들어온 이후부터 항상 믿어주시며 격려해주신 덕분에 이렇게 한걸음 더 나아가게 되었습니다. 믿음에 대한 보답을 해드리지 못한 것 같아 감사함보다 죄송함이 더 크지만 앞으로 정진하여 믿음에 꼭 보답하겠습니다. 그리고 부족한 저의 논문을 심사해주시고 많은 가르침을 주신 왕수균 교수님과 양민준 교수님께도 감사드립니다.

같이 프로젝트 하면서 많은 조언해주시고 곤란 할 때마다 항상 해결해주시는 김선옥 박사님, 학부생 때 부터 공실관에서 잘 챙겨주신 류호정 박사님께도 감사의 인사 드립니다. 실험실에서 같이 생활하면서 한 단계씩 나아갈수록 생기는 고민들에 대해 뜻깊은 조언을 해주시는 한이경 박사님, 다사다난했던 석사과정동안 느꼈던 희노애락 같이 나눌 수 있게 해준 소영이, 유나, 맨날 화만 내는 선배 실험 도와준다고 고생한 대현이, 정현이, 막내지만 배울 점 많은 민경이, 성실하고 우직한 우리 원범이, 4년 반 동안 실험실에서 좋은 추억 만들어준 선희, 현지, 경태, 눅짱, 경훈이에게 감사의 인사 드립니다. 또한, 부족한 후배들 챙겨주신다고 고생 많으신 진우선배, 인수선배, 항상 좋은 말씀만 해주시는 진영이형, 민호행님 1학년 때부터 따끔한 조언해주는 상희누나, 요즘 자주 못뵈서 죄송한 경배행님, 1학년 때부터 너무 멋있던 정택이형, 세윤이형, 힘든 시절 라면 나눠먹던 효진이누나 외에도 모든 선배들에게 감사의 인사드립니다. 같이 학교 다니면서 든든한 기웅이랑 창민이, 항상 욕으로 응원해주는 태형이, 진균이, 재원이, 동건이, 이현이 아빠 다빈이와 우리 동기 조아, 보정이, 원로 대학원생 병석이형, 취뽀 성공한 오상이에게도 감사의 뜻을 표합니다. 이번에 같이 졸업한다고 고생한 정훈이랑 호석이도 정말 수고 많았고 감사합니다.

항상 잘 되길 바라는 L1K4 (동윤, 태양, 현수, 찬영이)랑 취집 성공한 기특한 유부녀들 (수민이, 이슬이, 연재), 힘들 때 정말 힘이 되어 준 Starfish 30~32 (호수형, 명길이형, 석현이형, 준구, 성혁이, 병모, 윤성이, 지현이) 에게도 감사의 말씀 전합니다. 마지막으로 공부한다고 유난 떠는 못난 아들 낳아 주신 부모님과 언젠가 한번 한잔하고 싶은 형한테도 정말 사랑하고 감사하단 말씀 전하고 싶습니다.